Student thesis series INES nr 461

Analysis of the global ESA GlobPermafrost map for Scandinavia

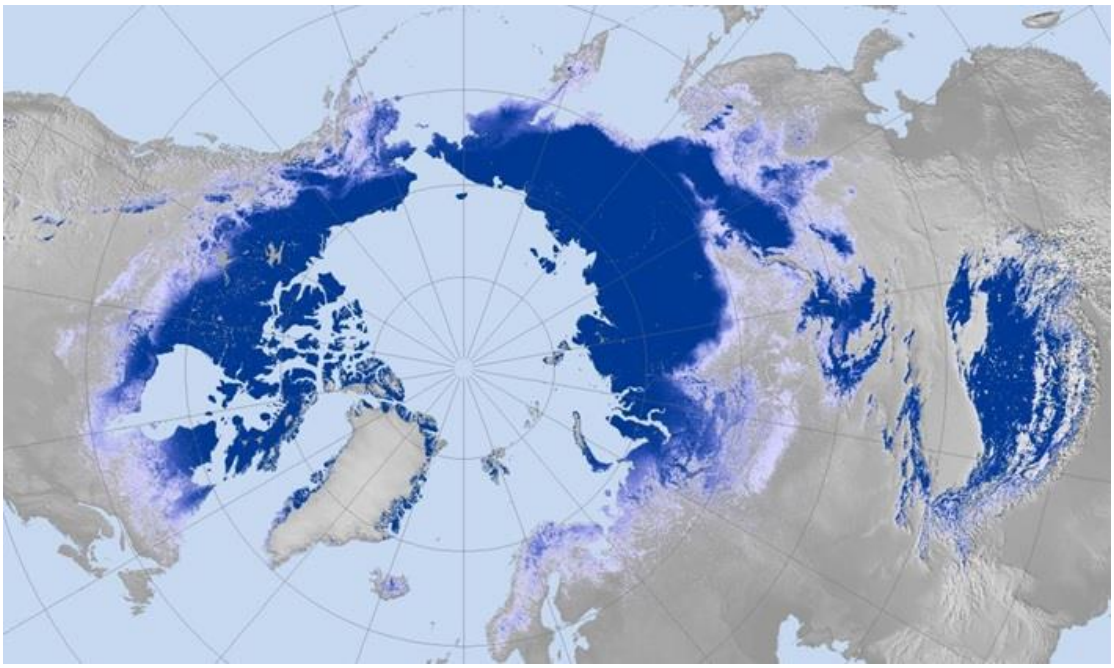

Nina Nesterova

2018

Department of

Physical Geography and Ecosystem Science

Lund University

Sölvegatan 12

Nina Nesterova (2018).
Analysis of the global ESA GlobPermafrost map for Scandinavia
Analys av den globala ESA GlobPermafrost kartan över Skandinavien
Master degree thesis, 30 credits in *Physical Geography and Ecosystem Analysis*
Department of Physical Geography and Ecosystem Science, Lund University

Level: Master of Science (MSc)

Course duration: *January* 2018 until *June* 2018

Disclaimer

This document describes work undertaken as part of a program of study at the University of Lund. All views and opinions expressed herein remain the sole responsibility of the author, and do not necessarily represent those of the institute.

Photographic credits:
Permafrost extent in GlobPermafrost map.

Obu, J., S. Westermann, A. Kääb, and A. Bartsch. 2018. Ground Temperature Map, 2000-2016, Northern Hemisphere Permafrost. PANGAEA. DOI:10.1594/PANGAEA.888600

Analysis of the global ESA GlobPermafrost map for Scandinavia

---

Nina Nesterova

Master thesis, 30 credits, in *Physical Geography and Ecosystem Analysis*

Sebastian Westermann, PhD
University of Oslo, Department of Geosciences

Margareta Johansson, PhD
Lund University, Department of Physical Geography and Ecosystem Science

Jaroslav Obu, PhD
University of Oslo, Department of Geosciences

Exam committee:
Marko Scholze, Lund University, Department of Physical Geography and Ecosystem Science
Paul Miller, Lund University, Department of Physical Geography and Ecosystem Science

ACKNOWLEDGEMENTS

"Every great achievement is but a small peak in the mountain range of contributions."
Dale T. Mortensen's speech at the Nobel Banquet, 10 December 2010

This thesis would not happen without help and support of the people I would like to thank below.

I am sincerely grateful for my main supervisor Sebastian Westermann to agree on heading the master project of the person he never met in person before, to trust, believe and take all risks related to that, to guide me during all the time, providing me with important and helpful comments and advices.

Thank you, dear Margareta Johansson, for liking this project from the beginning, for supporting me all the time, creating this positive and inspiring atmosphere, for being interested in my wellbeing and for tremendous help in final steps.

Dear Jaros, thank you a lot for your huge contribution, for your immediate help at all stages of the project, for your valuable comments and explanations which gave me insight of the model and the whole concept behind it.

I would also like to express my gratitude to my mom, dad, grandparents and M. for their love, care and support, even though it was remote, feeling this was very motivating.

Thank you my dear S., not only for that amazing day, but for believing in me, encouraging me and fully supporting me every day. I am genuinely happy to have you in my life.

I honestly appreciate huge contribution of J., his positive attitude, valuable comments, deep involvement in my topic and his incessant belief in my success, thank you for that.

Special gratitude should be expressed to all my Lund and not only Lund friends for being physically and/or mentally with me.

Thank you all different Capilatus inhabitants for your comments and help with my never ending difficulties.

I would like to also thank Frank Guenther, who did not personally take part in this project, but gave me a chance last summer to get closer to permafrost research and inspired me to keep going in this direction.

Last but not least I would also like to mention that this thesis as well as all my studies in Lund in general would never happen without a huge help from Russian government funding program "Global Education".

Thank you!

ABSTRACT

Due to its high vulnerability, permafrost is one of the key features studied in the field of climate change impacts. Permafrost is widespread in the Arctic region. The majority of the area underlain by permafrost is however difficult to access for in-situ monitoring and it is difficult to get an overview of the current state of permafrost in many areas.

Permafrost modeling provides a solution which overcomes this difficulty and allows studies on permafrost distribution as well as some characteristics, i.e. ground temperatures over large remote areas. Temperature at the top of the permafrost (TTOP) is one of several permafrost modeling approaches which conceptually represents a steady-state equilibrium model. In this study, two TTOP-based models were used; the GlobPermafrost model which was used to produce the most recent global permafrost map (Alfred-Wegener-Institut) and a local Scandinavian model.

The aim of this study was twofold; firstly, the performance of the GlobPermafrost model in Scandinavia was analyzed by comparing the model output with the output from the local Scandinavian model. Secondly, the role of land cover data as an input variable in the TTOP model was investigated. The TTOP-based GlobPermafrost model was run with different land cover input data to evaluate this.

In general, the GlobPermafrost model underestimated permafrost occurrence in Scandinavia (overall r^2 being 0.39). The lowest underestimation is located in the regions with little or no permafrost. The biggest underestimations are found in peatlands and mountainous areas with more likely permafrost occurrence. Unexpected underestimation of permafrost was observed in the forests. This exposed the weaknesses of regional permafrost model overestimating permafrost occurrence in forests.

The rerun of the GlobPermafrost model with three times more detailed land cover input data did surprisingly not have a great effect on the model performance (r^2 only changed by 8%). The small changes detected in the GlobPermafrost output could be explained by the changes in wetland fraction between the two land cover datasets used as input to the GlobPermafrost model.

The overall conclusions from this study are 1) that the GlobPermafrost model underestimates the amount of permafrost in the study area, especially in the mountains and 2) that improved input land cover data was only of minor importance to the TTOP model performance and future research should hence focus on other forcing input data to improve model performance.

Key words: *Physical Geography and Ecosystem analysis, Arctic, permafrost, permafrost modeling, TTOP, CryoGRID 1, GlobPermafrost, Scandinavia*

TABLE OF CONTENTS

1 INTRODUCTION

Permafrost underlies approximately a quarter of the Northern Hemisphere (Zhang et al. 2000) and it creates special living conditions for humans and ecosystems (Gruber 2012). Due to great vulnerability of permafrost to climatic fluctuations (Jorgenson and Grosse 2016) current and predicted climate change in the Arctic may lead to widespread thawing (Westermann et al. 2015b). Permafrost degradation results in various impacts in for example hydrology, infrastructure (i.e. slope instabilities leading to the damage or completely destroyed facilities), geomorphology (coastal erosion, landslides, rock falls, etc.), ecosystems (emissions of greenhouse gases from organic rich permafrost and change of species composition) (Gruber 2012).

Knowledge on the current state of permafrost, and especially its distribution and response to any change is important information for permafrost research. Harsh environmental conditions and low accessibility of remote permafrost areas are limiting the opportunities for field work to do permafrost monitoring and mapping permafrost extent. A global permafrost map developed by the International Permafrost Association (Brown et al. 1997) more than 20 years ago is still widely used (Westermann et al. 2015b) despite its coarse resolution and unknown uncertainty (Gruber 2012). Moreover, this map does not represent the heterogeneity driven by e.g. subsurface properties, land cover, topography, snow distribution, lateral variation, etc. (Gruber 2012).

Permafrost extent can be mapped using aerial photographs. However it is a method that can only be used at a local scale where permafrost landforms exist. Unlike other cryospheric components (snow, glaciers, lake and river ice), permafrost is not always visible in an area and hence it cannot be directly detected by optical satellite-based sensors (Zhang et al. 2014). However, there is a variety of characteristics available by remote sensing data which can indirectly contribute to assess the presence or absence of permafrost (Westermann et al. 2015a).

Application of such characteristics, i.e. satellite-based land surface temperatures (LST), can be employed in numerical permafrost models (Westermann et al. 2015a). Permafrost modeling can constitute the solution for different permafrost research limitations. Permafrost models provide an overview (Smith and Riseborough 1996; Gruber 2012; Gisnas et al. 2013; Zhang et al. 2014; Westermann et al. 2015b), translate subgrid variation of surface properties and result in fine resolution heterogeneous permafrost maps at different scales.

This study focuses on the most recent global model-based permafrost map published within the GlobPermafrost initiative of the European Space Agency. The GlobPermafrost permafrost map covers the circum-polar Arctic region. The aim of this project was twofold, firstly to investigate the performance of the GlobPermafrost map on a regional scale (for Scandinavia) by comparing the Scandinavian part of the GlobPermafrost map with a regional permafrost map developed by Gisnas et al. (2017) which was considered more trustworthy. Research questions associated with this aim were:

- *What is the uncertainty of the GlobPermafrost map when modeling a smaller geographical area such as Scandinavia?*

- *Where are the main mismatches located (if any) and what causes them?*

The second aim of this study was to evaluate the importance of different input land cover data for the performance of the GlobPermafrost model. Thus, key research questions were:

- *How will the result of the GlobPermafrost model output be affected if one of the model inputs – the land cover data (ESA CCI) will be replaced with more detailed land cover data (Corine 2012)?*
- *Where will the main changes be found and what causes them?*
- *What will the uncertainty of GlobPermafrost map be then?*

2 BACKGROUND

2.1 *Permafrost and permafrost landscapes*

Permafrost is defined as ground with temperatures at or below 0° C for two or more consecutive years (Brown et al. 1997). Permafrost is mostly found in alpine and polar regions (Brown et al. 1997).

Permafrost can be found in soil, peat, clay and even in bedrock (King 1986) and reach up to 1500 meters depth (Pidwirny 2006). The layer above permafrost that is characterized by seasonal thawing is called the active layer. The thickness of the active layer may vary from few decimeters to several meters (Network-CALM).

Permafrost landscapes are also commonly referred to as periglacial landscapes, where cold climate and the presence of frozen ground are the main characteristics. Dominant drivers of any permafrost dynamics are freeze-thaw actions (Pidwirny 2006).

Permafrost is classified in different zones (Baranov and National Research Council of Canada. Division of Building 1964; Brown et al. 1997; Gisnas et al. 2017) determined by the percentage of area underlain by permafrost. The International Permafrost Association defined permafrost occupying more than 90% as continuous, 50% - 90% of permafrost area as discontinuous, 10 - 50% as sporadic permafrost and 0-10% as isolated islands (IPA). Discontinuous permafrost is found at the margins of continuous permafrost and represents a transitional zone. Sporadic permafrost and isolated islands stand for patches of permafrost surrounded by unfrozen ground (Pidwirny 2006).

2.2 *Study area*

The study area is defined by the administrative borders of Norway, Sweden and Finland. In the following text, it will be referred to as Scandinavia, Scandinavian Peninsula or Fennoscandia for simplification even though neither of these definitions is completely correct.

2.2.1 Physical geographical description

The geology of the Scandinavian Peninsula is mostly dominated by Precambrian bedrocks: granite and gneisses (Lidmar-Bergström and Näslund 2005). The Scandinavian Mountains (the Scandes) located at the western part of the peninsula, were formed in Caledonian orogeny. Topographically relief of Fennoscandia can be divided into lowlands and uplands and Scandes.

Despite the dominance of Precambrian bedrock in Fennoscandia, there are significant differences within a relative relief of lowlands and uplands. It consists of 1) exceptionally flat *sub-Cambrian peneplain* (<300 m a.s.l), occupying south central Sweden and Finnish west coast, 2) *structurally controlled landscape* (20-50 m a.s.l.), occurring in southern Finland and the area around Stockholm, 3) *undulating hilly terrain of etch character* (20-100 m a.s.l.), covering south-eastern Norway and central Sweden and 4) other *plains with residual hills* of 200-500 m a.s.l. and 100-150 m a.s.l. (Lidmar-Bergström and Näslund 2005). The relief of the Scandinavian Peninsula was significantly modified by multiple glaciations. Thus, expositional and erosional landforms are common geomorphological features in the area.

The climate in the study area ranges from a so called Cfb-climate (according to the Koppen-Geiger-Pohl system) in the southernmost part of the area to ET in the northernmost part, while majority of the study area belongs to the Dfc-climate (Tikkanen 2005). Mean annual air temperature of the region is around 9° C but locally it can be as low as – 5° C in the highest parts of the Scandinavian mountains (Gisnas et al. 2017). The main climatic (precipitation in particular) differences within the study region are caused by the warming effect of the Gulf Stream on the west coast and by the Scandes which act as an orographic barrier and lead to much more continental conditions to the east of the mountains (Tikkanen 2005).

The vegetation in the study area can be defined as the nemoral zone in the southernmost parts of Sweden, the boreonemoral zone occupying the majority of southern Sweden and southern coast of Finland. The southern boreal zone is characteristic for a narrow belt in central Sweden, western coast of Norway and the majority of southern Finland. The middle boreal zone covers the majority of the central and the northeastern part of Sweden and central Finland. The northern boreal zone is found in the northernmost parts of Sweden, Norway and Finland, and also in the Scandinavian mountain range where it neighbors the alpine zones at high elevations (Anonymous 2014).

2.2.2 Permafrost in Scandinavia

Permafrost in Fennoscandia can generally be characterized as sporadic and discontinuous permafrost. Thus, the region can also be referred to as a marginal zone of permafrost (Seppälä 2005).

Most of the permafrost in Scandinavia is located in the mountains (Etzelmuller et al. 2003; Seppälä 2005; Gisnas et al. 2017) and the belt of high altitude permafrost was classified by King (1986) as continuous. In terms of vertical zonation of permafrost in the mountains, the continuous permafrost is followed by discontinuous and sporadic permafrost. The thickness of mountain permafrost can reach more than 350 meters (e.g. in Tarfalaryggen; (Isaksen et al. 2001)) in the study area.

In the northern non-mountainous part of Fennoscandia, permafrost is mainly found in palsa mires and peat plateaus (King 1986; Johansson et al. 2006; Gisnas et al. 2017) but can also be found in ice-cored moraines and pingo-like frost mounds (Seppälä 2005).

2.3 *Permafrost modeling*

Permafrost is widespread in the Northern Hemisphere and some of the areas are difficult to access. The numbers of observations are sparse especially in certain areas and hence permafrost modeling is needed to understand the distribution of permafrost at a larger scale. Model-based maps present detailed information on the permafrost extent and ground temperatures for a certain area. The fundamental principle of permafrost models is to use indirect parameters or indices in nature that leads to the conclusion of permafrost presence or absence in a certain area.

The importance of using indirect indices to define areas of permafrost occurrence was emphasized already in 1959 by Baranov. It was stated that there are two important climatological indices used to define the area of permafrost based on air-soil temperature relationships. The first

index consisted of January mean air temperature in Northern Hemisphere and July mean air temperature. The second index was described as the time duration of freezing temperatures. This parameter together with mean air January temperature are widely implemented in further permafrost modeling studies and particularly in "temperature at the top of the permafrost" (TTOP) modeling approach (Smith and Riseborough 1996; Gisnas et al. 2013; Westermann et al. 2015b; Gisnas et al. 2017).

Temperature at the top of the permafrost approach (TTOP) belongs to equilibrium permafrost models. The main assumption of such models is the equilibrium relations of ground thermal properties with a climate. Equilibrium permafrost models are considered to be simple and with low input data requirements. They are widely used to estimate active layer thickness, the temperature at the upper permafrost layer and to project permafrost occurrence (Callaghan et al. 2011).

Transient modeling approach is another concept within permafrost modeling which simulate dynamic transient response of permafrost ground properties to the changing climate. This approach is more advanced and require complicated calculations and the big number of inputs (Callaghan et al. 2011).

In this study results of two applications of CryoGRID 1 model based on TTOP approach are investigated.

2.3.1 TTOP modeling approach and CryoGRID 1 model

The main concept of the CryoGRID 1 model used in this study is based on the top of the permafrost (TTOP) equilibrium modeling approach developed by Smith and Riseborough (1996). The TTOP model applies annual freezing and thawing degree days as major factors of atmospheric-climate and ground relationships. Estimates of temperatures at the top of the permafrost can be obtained as follows (Smith and Riseborough 1996):

$$\mathrm{TTOP} = \frac{k_T * N_T * DDT_A - k_F * N_F * DDF_A}{k_F * P} \qquad (1)$$

where

k_T = thermal conductivity of thawed ground (W m^{-1} K^{-1})
k_F = thermal conductivity of frozen ground (W m^{-1} K^{-1})
N_T = thawing N-factor
N_F = freezing N-factor
DDT_A = air thawing degree days (number of days)
DDF_A = air freezing degree days (number of days)
P = time period (365 days)

N-factors represent semi-empirical transfer functions which account for air-ground surface temperature offsets. These functions combine important environmental factors such as vegetation, snow cover, soil moisture and topography (Gisnas et al. 2017).

2.3.2 Regional Scandinavian permafrost model

The permafrost map for Norway, Sweden and Finland (hereafter called regional Scandinavian permafrost map) developed by Gisnas et al. (2017) is based on the TTOP approach.

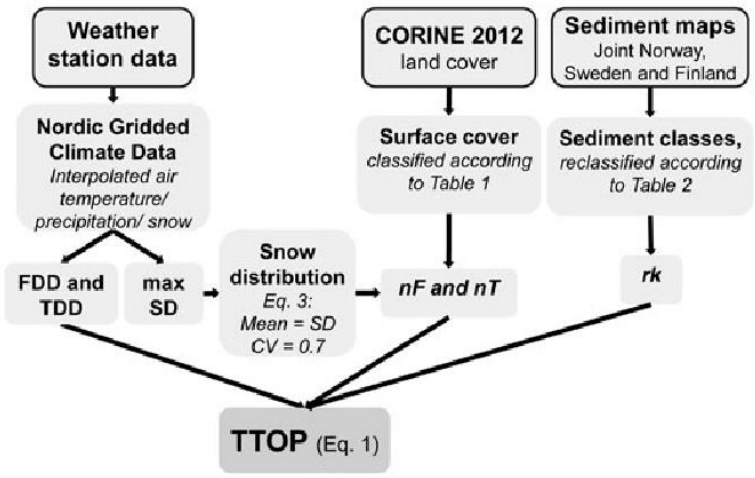

Figure 1 Scheme of regional permafrost model set-up (Gisnas et al. 2017). FDD – freezing degree days, TDD – thawing degree days, SD – snow distribution, CV – coefficient of variability, nF- freezing n-factors, nT – thawing n-factors, rk –ratio of thermal conductivities. Access permission: John Wiley and Sons license # 4355821229240. Note, that equations and tables referred in this figure are related to the original study.

K-values of thermal conductivity (Equation 1) are replaced by rk-values which represent ratio of thermal conductivities of thawing/frozen ground. Values of rk were specified based on sediment maps of the study area (Olesen et al. 2010).

Freezing and thawing degree-days were estimated from air temperature data from Nordic Gridded Climate data (Norwegian Meteorological Institute, Oslo).

N-factors (Equation 1) for the Gisnas et al. (2017) model were acquired by using Nordic Gridded Climate data together with Corine land cover 2012 (Aune-Lundberg and Strand 2010) (Figure 1). Freezing and thawing N-factors for vegetated areas were assigned based on land cover classes of Corine land cover 2012 (Aune-Lundberg and Strand 2010). Freezing N-factors for non-vegetated areas as well as thawing n-factors were obtained by applying empirical equation describing its relationships with snow depth.

Probability density function of snow depth (Skaugen et al. 2004) was applied using fixed coefficient of variability (CV=0.7) and average maximum snow depth of the grid cell derived from climatic data. Different snow depths were selected from snow depth probability distribution to run 100 model realizations. Thus, freezing n-factors for non-vegetated areas and thawing n-factors were calculated for each run.

TTOP model was run for each grid cell. The result of the TTOP model is a distribution of temperatures at the top of the permafrost per every cell. Based on this distribution percentage of sub-zero temperatures were estimated per every cell. This percentage was also used by Gisnas et al. (2017) to classify the area underlain by permafrost. Thus, the fraction of sub-zero temperatures at the top of the permafrost predicted by the model was grouped by IPA permafrost occurrence classification: >90% - continuous, 50-90% - discontinuous, 10 - 50% - sporadic and 0-10% - isolated islands.

The result of the model was compared to the temperature measurements in the field and landforms observations. Evaluation of the model showed a fairly good performance of the model (with accuracy of 100 m), which makes it reasonable to assume that the resulting map of this model can represent the true permafrost distribution in Scandinavia.

There are several outcomes of this model, however, in this study we focus on the map representing permafrost fraction (in other words, permafrost probabilities or percentages). The regional permafrost map of Scandinavia is initially in a form of a raster file with 1000 meters resolution and in ETRS 1989 LAEA projection. The values of each raster cell vary from 0.0 to 1.0. The scope of the map is restricted to the boundaries of Norway, Sweden and Finland.

2.3.3 GlobPermafrost map model

The "GlobPermafrost" permafrost map was developed in 2017 within the GlobPermafrost initiative of the European Space Agency covering the circum-Arctic region. The GlobPermafrost model also applies the CryoGRID 1 model (section 2.3.1), thus is similarly based on the TTOP approach.

To calculate the freezing and thawing degree days, land surface temperatures derived from the Moderate Resolution Imaging Spectroradiometer (MODIS) Terra and Aqua satellites were applied. 104 MODIS tiles were used covering an area of 1200*1200 km for a period from 1.1.2000 to 31.12.2016. Data gaps due to clouds were filled with ERA-interim air temperature data, which were downscaled to MODIS pixels using air temperature lapse rates calculated with digital elevation model (GMTED 2010) (Obu et al. in prep.). A similar approach was used and is well described by Westermann et al. (2015b) to estimate freezing and thawing degree in the North Atlantic permafrost region.

Thawing n-factors were omitted in this model since thawing degree days represent ground surface and no transfer function from air temperatures is required (Westermann et al. 2015b). Freezing n-factors were computed based on the function developed by Smith and Riseborough (1996) that describes the relationship between freezing n-factors, snow depth and mean annual air temperatures. Snow depth was in turn calculated from snow water equivalent (SWE) and snow density that was estimated from mean January temperatures and snow cover duration as described by Onuchin and Burenina (1996). Snow water equivalent as well as snow cover duration was computed with a snowfall model where ERA-interim air temperature and precipitation data were downscaled using GMTED 2010 digital elevation model (Obu et al., in prep.). Mean January temperatures were acquired from MODIS land surface temperatures (LST) together with the ERA-interim air temperature data. Fig 2 depicts the conceptual model of GlobPermafrost and describes the freezing n-factor calculations in more details.

Ratios between thawed and frozen ground (rk-values) were defined based on two datasets. Tundra wetness data published by Widhalm et al. (2016) were used to assign rk-values since ice content of the soil is a main cause of difference in thermal conductivities (Westermann et al. 2015b). The rk-values were 0.75, 0.85 and 0.95 for wet, medium and dry tundra wetness classes. The rest of the area, which was not covered by these classes (i.e. open, shrub, forest, wetlands,

water land cover classes of ESA CCI land cover map (2008-2012, v. 1.6.1)), were grouped and a set rk-value was applied (Obu et al., in prep.).

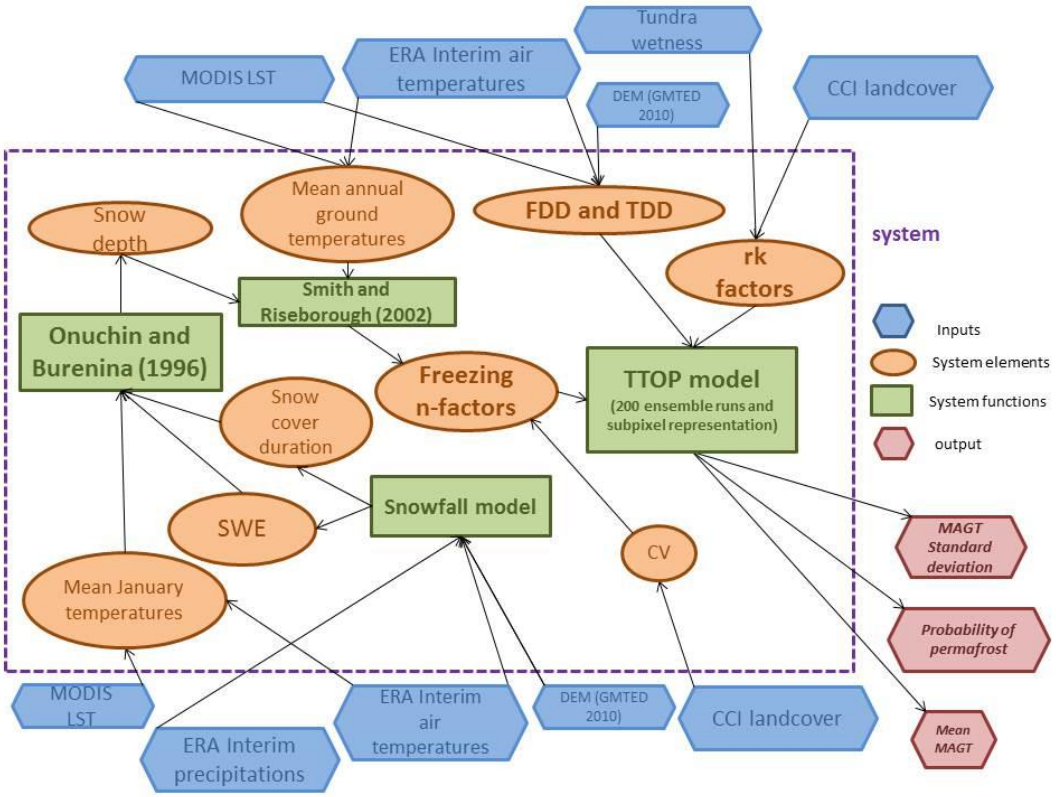

Figure 2 Conceptual model of GlobPermafrost (modified from Obu et al. in prep.). FDD – freezing degree days, TDD – thawing degree days, SWE – snow water equivalent, CV – coefficient of variability, rk factors – ratio of thermal conductivities, MAGT – mean annual ground temperatures.

The ensemble run was conceptually similar to the one described for regional Scandinavian permafrost model. Two hundred runs with different rk-values and nf-factors combinations were performed including sub-pixel variability for snow and ground properties (Obu et al. in prep.). Sub-pixel variability was estimated by computing proportions of every land cover class per cell of MODIS grid.

Coefficient of variability (CV) was assigned based on ESA CCI land cover classes. Areas with water bodies and glaciers were masked out in this model (Obu et al. in prep.).

The fractions of model runs with subzero mean annual ground temperatures were estimated per every grid cell. These fractions were also used by Obu et al. (in prep.) as percentages of permafrost occurrence in the area (or probabilities), thus can be also grouped by IPA classification.

The outputs of the GlobPermafrost model, in particular mean annual ground temperatures were validated by comparison with in-situ Global Terrestrial Network for permafrost and Thermal state of permafrost borehole datasets. The performance of the GlobPermafrost model was assumed satisfactory (Obu et al. in prep.).

The GlobPermafrost map (with permafrost probabilities) has a raster format with 926 meters resolution of cells projected in WGS 1984 Arctic Polar Stereographic. The map covers the Northern Hemisphere.

3 DATA AND METHODS

3.1 Performance of GlobPermafrost map at the regional scale of Scandinavia

To compare the performance of the Globpermafrost model in Scandinavia with the results of the regional permafrost model for Scandinavia, the two maps needed to be aligned. To be able to carry out the comparisons the following steps were taken:

- Firstly, a raster file of the permafrost map of Scandinavia was vectorized dissolving all values into 1. This map was then reprojected to WGS 1984 Arctic Polar Stereographic so the values corresponding to the study area could be extracted from the GlobPermafrost map.
- Secondly, the regional permafrost map of Scandinavia was reprojected from ETRS 1989 LAEA projection to WGS 1984 Arctic Polar Stereographic and downscaled from 1000 m to the resolution of 926 m to fit the resolution of the GlobPermafrost map. The loss of variance after this transformation was 2.82%.
- The extents of both maps were set up to align.

Both initial and after rerun comparisons were based on basic raster analysis including extraction, overlay and cross plotting. The results of the analysis were also compared to Corine land cover (2012) classes.

3.2 Rerun of GlobPermafrost model with Corine land cover

To evaluate the importance of land cover input data, the GlobPermafrost model was rerun using Corine land cover data (resolution 100 m) as an input instead of CCI land cover data (resolution 300 m). Setups of the rerun are following initial setups described in section 2.3.3.

The two parameters of GlobPermafrost, which are affected by land cover data, are the coefficient of variability (CV) for snow and ground properties and the rk-factors. Thus, the rk-values and the freezing n-f factors are two TTOP-model inputs which were eventually modified.

In GlobPermafrost values of thermal conductivity ratios were assigned to groups of land cover classes (Obu et al. in prep.). The grouping of Corine land cover classes was performed in a similar way as the grouping of ESA CCI land cover classes. The same values of rk-factors were assigned to groups of Corine land cover classes (Table 1).

Values of the coefficient of variability (CV) for sub-pixel representation applied in TTOP function of the GlobPermafrost model (Fig. 2) were also assigned based on ESA CCI land cover classes. Groups of CV were defined by the height of the vegetation as follows: open, shrubs, forest, wetlands and water (Obu et al. in prep.). CV groups correspond to rk reclassification groups as it is shown in Table 1. For the rerun of GlobPermafrost model, CV-values were assigned to rk reclassification groups containing Corine land cover classes.

Subcell statistics defining subcell variability in the model (as described in section 2.3.3) were also estimated based on Corine land cover map.

Table 1 Assignment of rk-factors (ratios of thermal conductivities) and CV values (coefficient of variability).

Rk-factors assignment in GlobPermafrost			
Group	CCI land cover classes grouped	rk-value	Corine land cover classes grouped
bare areas	140, 150, 152, 153, 200, 201, 202	0.8	322, 331, 332, 333, 334, 335
grasslands and croplands	10, 11, 12, 20, 130	0.75	211, 213, 222, 231, 242, 243, 321, 212, 221, 223, 241, 244
shrubs	30, 40, 100, 110, 120, 121, 122	0.8	323, 324
forests	50, 60, 61, 62, 70, 71, 72, 80, 81, 82, 90	0.95	311, 312, 313
wetlands	160, 170, 180	0.55	411, 412, 421
urban areas	190	0.7	111, 112, 121, 122, 123, 124, 131, 132, 133, 141, 142
water bodies	210	-	423, 511, 512, 521, 522, 523, 422
Coefficient of variability (CV) assignment			
CV group	Land cover class groups from rk reclassification		Value
open	bare areas, grasslands and croplands, urban areas		0.9
shrubs	shrubs		0.4
forests	forest		0.2
wetlands	wetlands		0.4
water bodies	water bodies		0.4

3.3 Software

Majority of data analysis was performed in RStudio Version 3.4.3 (2017-11-30) and ArcGIS Desktop 10.5 (version 10.5.0.6491). Rerun of the model was carried out in Matlab R2017a

(9.2.0.556344). Subcell statistics were estimated using arcpy library of Python 2.7 in Spyder 2.3.9 (The Scientific PYthon Development EnviRonment). Some graphs and tables were also produced in Microsoft Excel Version 14.0.4760.1000.

4 RESULTS

4.1 Performance of GlobPermafrost map at the regional scale of Scandinavia

4.1.1 Initial comparison

Model output from the GlobPermafrost and regional permafrost models are depicted in Figure 3.

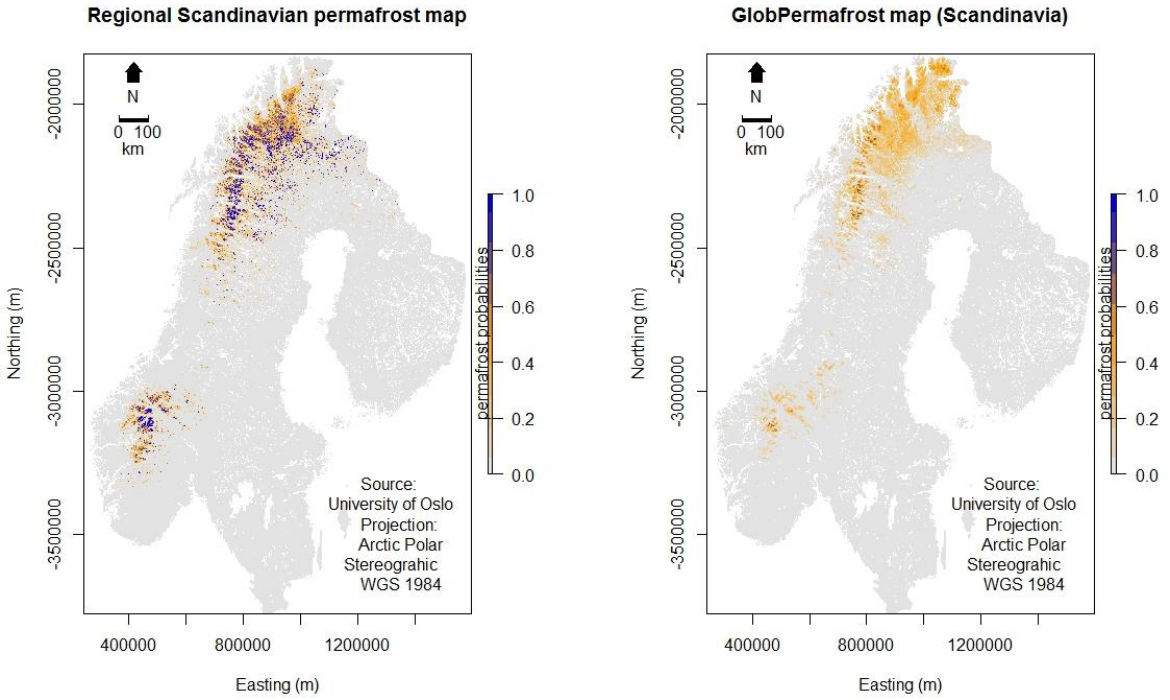

Figure 3 Permafrost distribution in the study area according to the regional permafrost model (left) and the GlobPermafrost model (right). Color axis: modeled probability of permafrost occurrence within 1 km pixels with values between 0 (no permafrost) and 1 (complete coverage).

The regional model shows significantly bigger variety of fraction of the grid that is underlain by permafrost values (permafrost probability) compared to the GlobPermafrost. Continuous occurrence of permafrost (where permafrost probability is close to 1) can be found in the mountainous and northern part of Scandinavia in the regional map. On the contrary, the GlobPermafrost map only predicts very little continuous permafrost.

This is also illustrated in Figure 4, which depicts histograms of values of the two maps. Values <0.1 were excluded from the analysis since their dominance on both maps caused significant right skew (original data had a value higher than 4). Distribution of GlobPermafrost map values is strongly right skewed; the histogram is unimodal with a peak at very low values with an exponential decrease. The GlobPermafrost map is showing significantly less of high permafrost probabilities (such as >0.8), which is also illustrated in Figure 3.

The shape of the distribution of permafrost probability values (>0.1) in the regional map greatly differs from the GlobPermafrost map. On the histogram with values >0.1 four modes (peaks) can

be found. One of the modes belongs to high values around 1.0 permafrost probability. This high variety of values in regional map compared to GlobPermafrost can be also noticeable in huge difference of variance, which is approximately 75%, as well as in much higher dispersion with 2 times difference between standard deviations.

However, certain similarities can also be found when comparing the two maps: the median values of both maps are 0.0 and the mean values' difference is 1.6 times (Fig. 4).

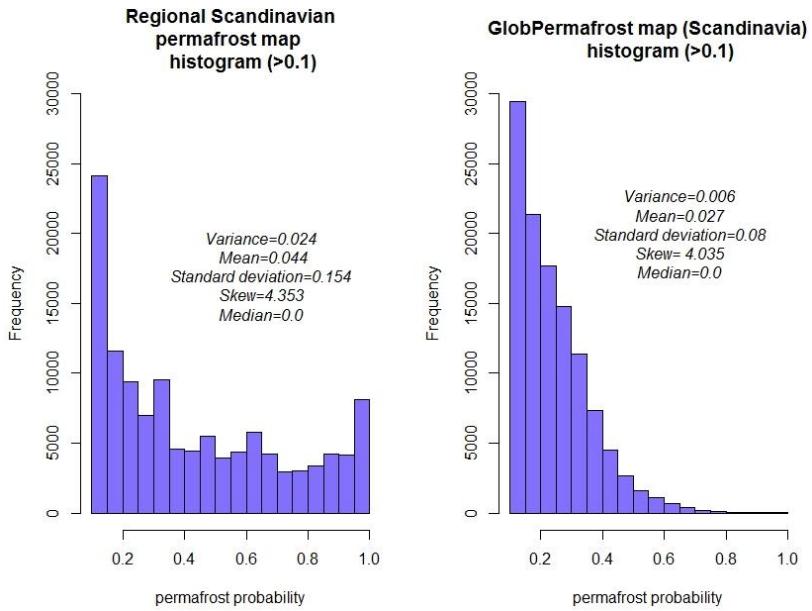

Figure 4 Distribution of permafrost probabilities (higher than 0.1) in the regional permafrost map (left) and the GlobPermafrost map (right). Note that statistical parameters in the graphs describe the original data with all range of values of permafrost probability: from 0.0 to 1.0.

In this study we assume that the result of the regional permafrost model is closest to the reality (Gisnas et al. 2017), and hence the regional permafrost map was used to validate the performance of the GlobPermafrost map. The relationship between these two maps is depicted in Figure 5.

In general, the distribution of the values in the scatterplot does not follow the 1:1 line trend which means that the permafrost distribution is quite different in the two maps. The GlobPermafrost map is in general underestimating the permafrost probability. The underestimation rises with increasing permafrost probability in the regional map. The variation of the GlobPermafrost estimations has the same rise with permafrost.

The best fit between the two models occurs at low permafrost probabilities. The best performance of the GlobPermafrost map can hence be found for no permafrost areas or for areas with sporadic permafrost, which are the most common types in study area (Fig. 3).

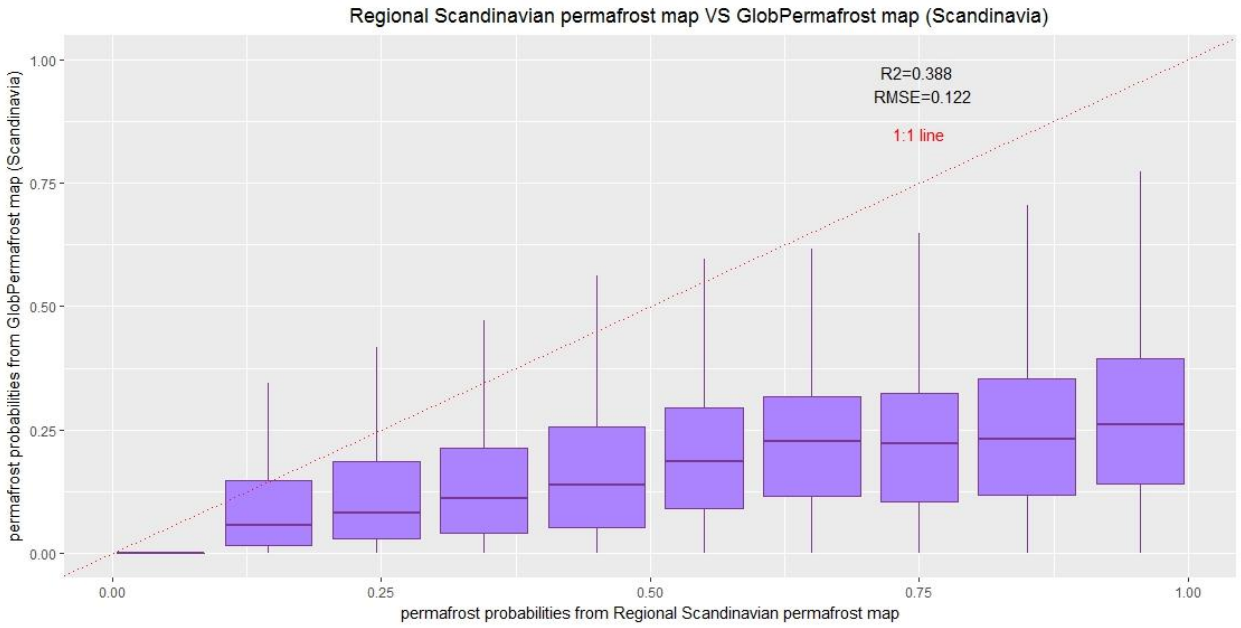

Figure 5 The relationship between permafrost probability in the regional permafrost map and the GlobPermafrost map. Outliers are masked out in this plot. Purple boxes represent 75% of the data, horizontal line within boxes represents the median (50% of the data). Purple bars represent variation and their tips show the greatest and the lowest values without outliers, note that bars do not represent errors.

The root mean square error of the GlobPermafrost map compared to the regional map is relatively small. Coefficient of determination (r^2) equals to 0.38, which means that almost 40% of the variation in the regional permafrost map is described by GlobPermafrost map.

Differences between the GlobPermafrost and the regional maps were estimated and plotted (Fig. 6). Since simple extraction of one map from the other may lead to values equal to 1 on both maps which would cancel each other when plotting a difference map, we used a non-zero approach. The non-zero approach included extracting non-zero values of one map from the initial values of the other map and vice versa. Particularly in this map, non-zero values of GlobPermafrost map were extracted from the regional permafrost map. Areas with positive values of non-zero differences represent regions where there is more permafrost in the regional map than in GlobPermafrost. Vice versa, areas with negative values of non-zero differences show regions where there is more permafrost in the GlobPermafrost than in the regional map.

A threshold of 10% differences was applied, so only differences lower than -0.1 and higher than 0.1 are presented. Pixels representing glaciers and perpetual snow were excluded from Figure 6, since they were masked out and not accounted in the GlobPermafrost model, but were applied in the regional permafrost model.

Positive differences in Figure 6 are mostly located in the mountains, both in the northern and southern parts. The distribution of the positive differences is highly dispersed with values ranging from 0.1 to 1. This corresponds to the high variation found in the regional map values described above. On the contrary, the dispersion of negative differences (i.e.) is much lower. The shape of the histogram is more leptokurtic and the lowest value of negative difference reaches -0.88. The

majority of the negative differences are located in the North (where most of permafrost can be found in the study region) both in the mountains as well as in lowland wetland areas.

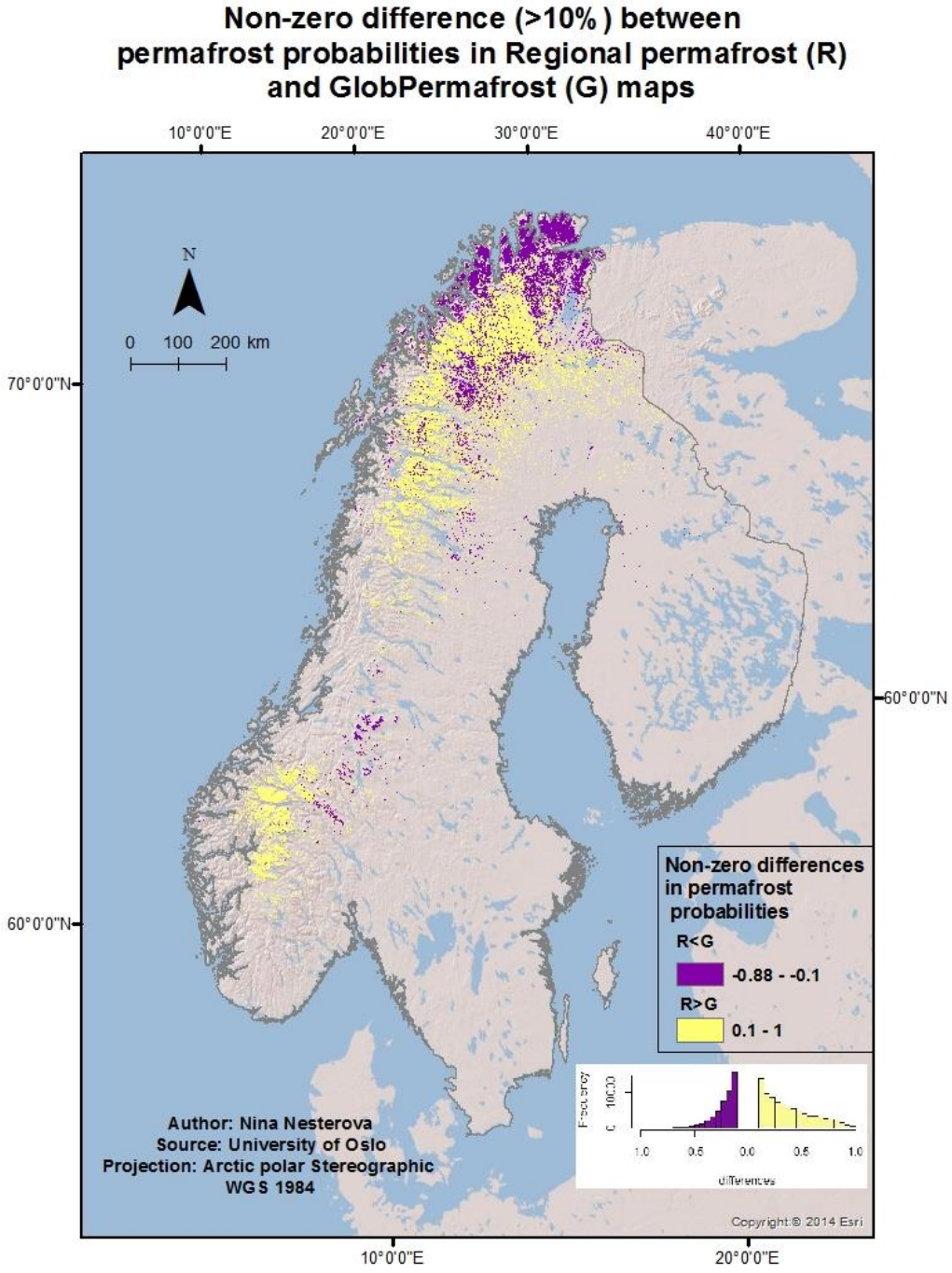

Figure 6 Map of the study area showing areas of differences (>10%) between the regional permafrost map (R) and the GlobPermafrost map (G). Yellow denotes positive differences where there is more permafrost in the regional map than in GlobPermafrost. Purple indicates negative differences where there is more permafrost in GlobPermafrost map. Histogram depicts the distribution of positive and negative differences.

4.1.2 Performance of GlobPermafrost map compared to Corine land cover classes (2012)

Differences between the regional permafrost map and the GlobPermafrost map were compared with land cover of these areas. Land cover representation of differences is shown on Fig. 7. Both differences (negative and positive) shown in Figure 6 are mostly located in sparsely vegetated areas, peat bogs, moors and heathland. It represents 75% of the area of negative differences and 67% of the areas of positive differences. Approximately the same amount of both positive and negative differences occurs in forests: 17% (broad-leaved and coniferous forests) for positive differences (Fig.7, left) and 18% (broad-leaved, coniferous and mixed forests) for negative differences (Fig. 7, right).

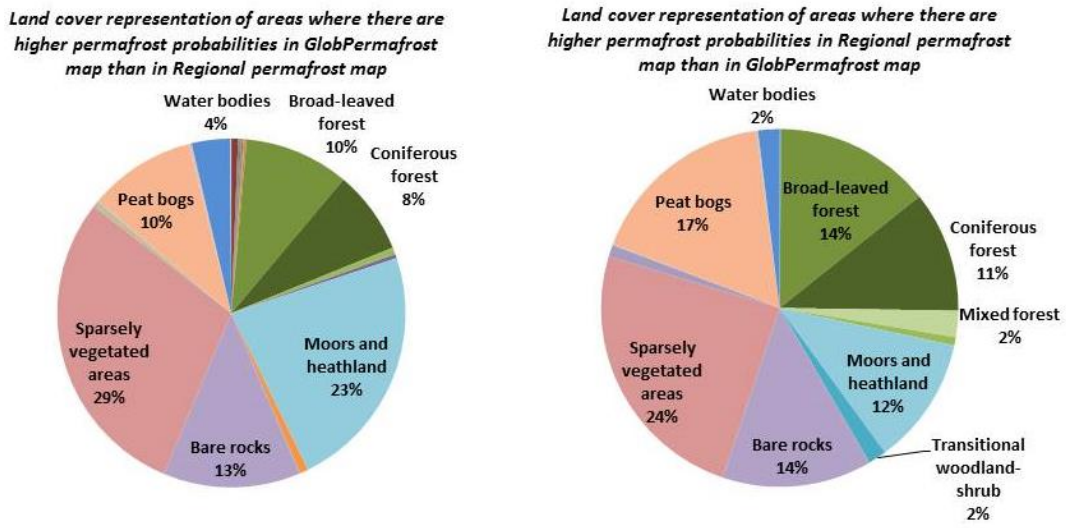

Figure 7 Land cover representation of areas where there is more permafrost in GlobPermafrost map than in regional permafrost map (left) and areas where there is more permafrost in regional permafrost map than in GlobPermafrost map (right).

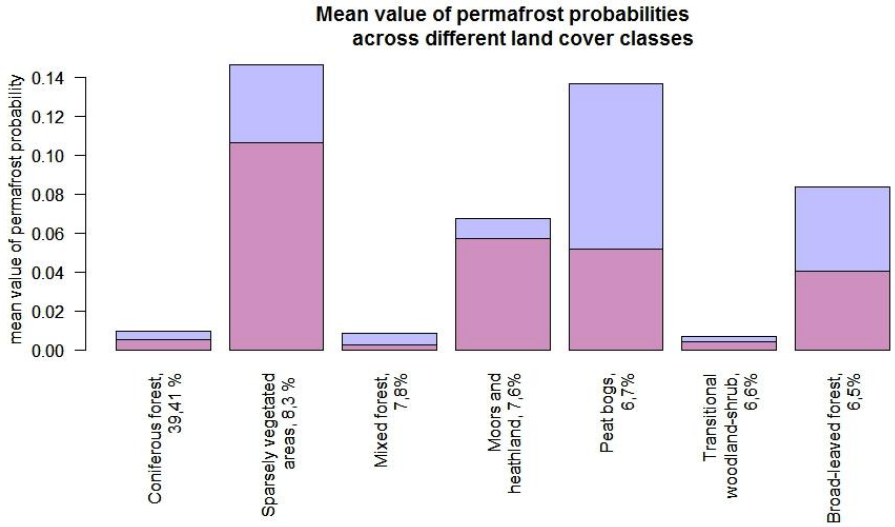

Figure 8 Mean value of permafrost probability per land cover class. Blue bars represent mean values of permafrost probabilities in regional permafrost map. Pink bars show mean value of permafrost probabilities in GlobPermafrost map. Note, that bars overlap.

In the regional permafrost map, permafrost is most likely in sparsely vegetated area land cover class and in peat bogs. In the GlobPermafrost map, mean value of permafrost probability is also the highest for sparsely vegetated areas, peat bogs and moors and heathland have relatively same second highest mean value. Both peat bogs and sparsely vegetated areas land cover classes have the highest variance of permafrost probabilities among other land cover classes in the regional permafrost map as well as in the GlobPermafrost map (Table 2).

Table 2 Variance of sparsely vegetated areas and peat bogs in the regional and the GlobPermafrost maps.

Variance		
	Sparsely vegetated areas	**Peat bogs**
Regional permafrost map	0.064	0.074
GlobPermafrost map	0.019	0.007

Values from the map of the study area showing areas of differences between the two permafrost maps (the regional map and the GlobPermafrost map; Figure 6) were extracted for each land cover class that covered more than 5% of the study area (Fig.9). All histograms show similar shapes of distribution with peaks around 0.0. The highest variance of differences can be found for sparsely vegetated areas and peat bogs, which corresponds to original values in Table 2. The highest mean and maximum values of differences are also found in sparsely vegetated areas and peat bogs, where permafrost is expected to occur. The lowest mean and minimum values8 of difference are found in classes where permafrost probabilities are initially lower.

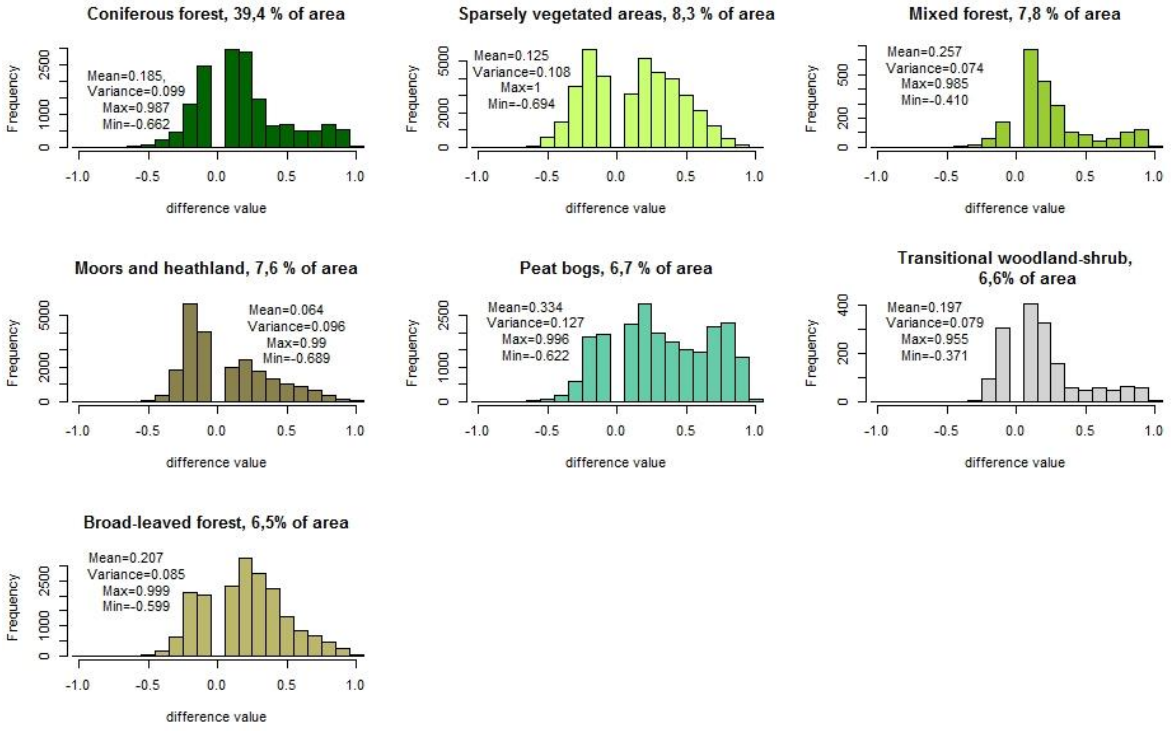

Figure 9 Distributions of differences in permafrost probabilities between regional permafrost map and GlobPermafrost map among different land cover classes (note different scale). Frequency shows the number of 1km pixels in the respective bin of difference values.

Different statistical parameters are shown in Figure 10. The highest r^2 are found in sparsely vegetated areas and peat bogs. This means that the GlobPermafrost map explains variety of permafrost probabilities of regional map in these land cover classes better than in other. This can be explained by initially highest values of variance in these land cover classes in both maps (Table 2). Different errors among land cover classes also reach their maxima at peat bogs and sparsely vegetated areas. This confirms that classes where there is no permafrost correspond to no permafrost in the model as well and thus the lowest variance, lowest mean and variance of differences and lowest errors.

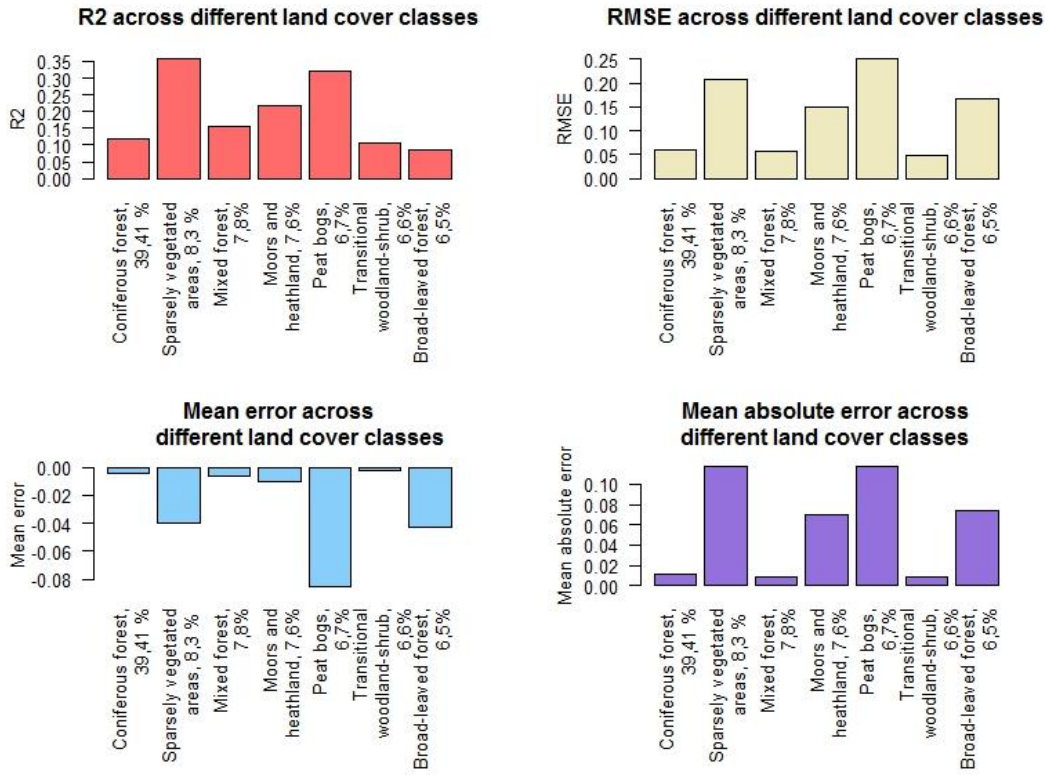

Figure 10 Statistical parameters of GlobPermafrost performance for different land cover classes. Units of errors (RMSE, mean error, mean absolute error) are permafrost probabilities.

4.2 Influence of Corine land cover on GlobPermafrost

A comparison of the original GlobPermafrost map using the CCI land cover map with the GlobPermafrost map after the rerun of the model using the Corine land cover map is presented in Figure 9. Visually the maps look quite similar. The performance of the GlobPermafrost compared to the regional permafrost map differs around 2%: the original r^2 of GlobPermafrost map equals to 0.38 and the r^2 after the rerun of the GlobPermafrost map equals to 0.36.

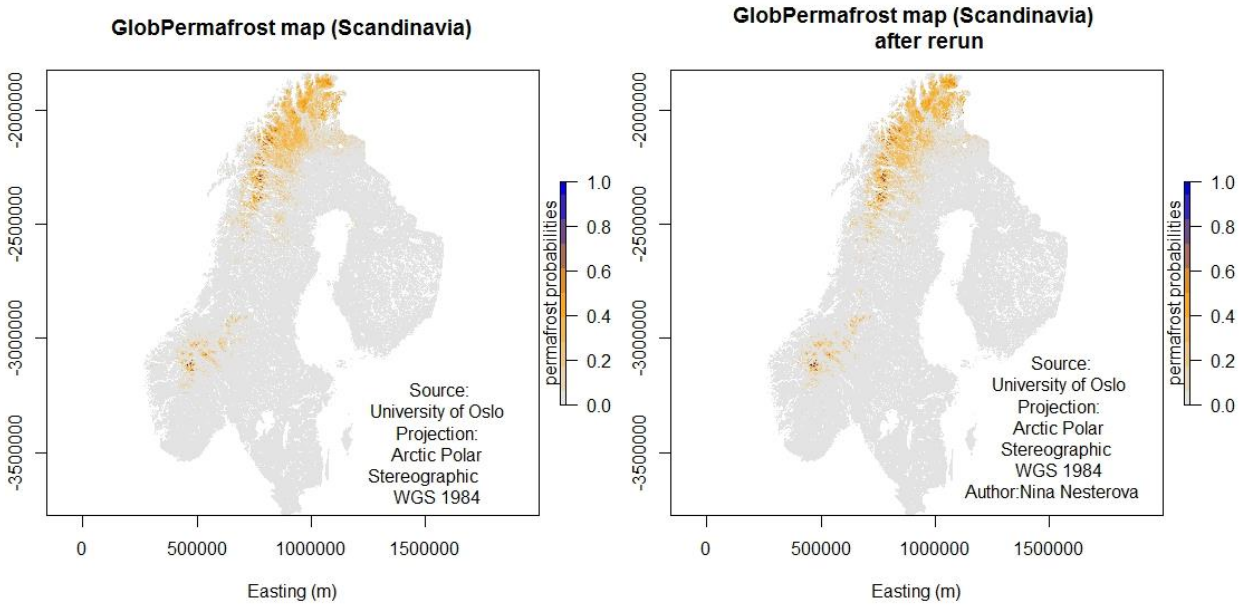

Figure 11 Original GlobPermafrost map in Scandinavia (http://maps.awi.de/map/; left) and GlobPermafrost map in Scandinavia after rerun of the model using Corine 2012 land cover map (right).

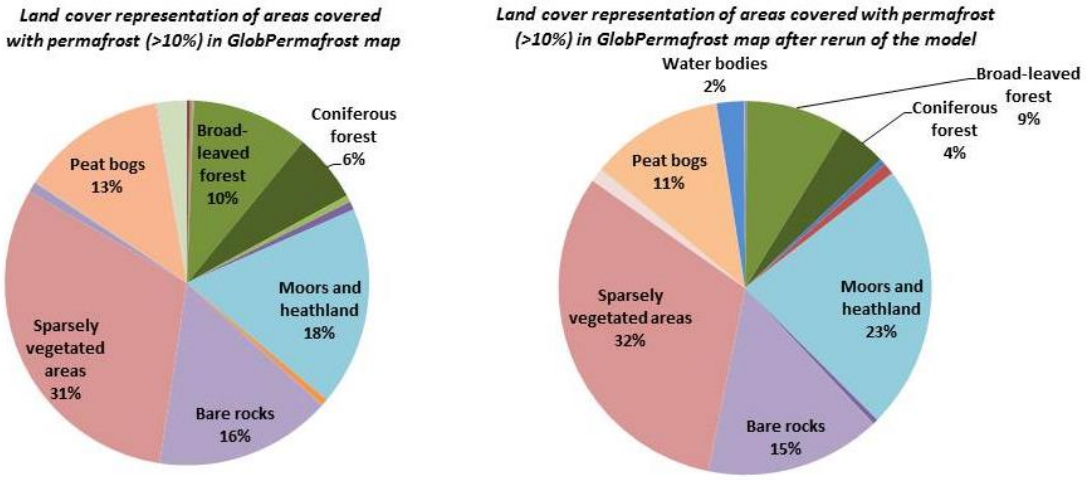

Figure 12 Land cover representation of areas with permafrost (probabilities higher than 0.1) in the GlobPermafrost map before (left) and after the rerun (right) of the model.

The proportions of land cover classes in the GlobPermafrost map before and after the rerun were very similar (Fig. 12).

The same non-zero approach (as described above) was used to estimate differences between the original and the rerun version of the GlobPermafrost map (Fig. 14). The same threshold of 10% was applied, thus only cells with differences more than 0.1 permafrost probability or lower than -0.1 are shown on the plot. The majority of the differences (both positive and negative) are located in the north. Histograms of the negative and the positive differences look quite similar, which means that approximately the same amount of permafrost probabilities were gained and lost.

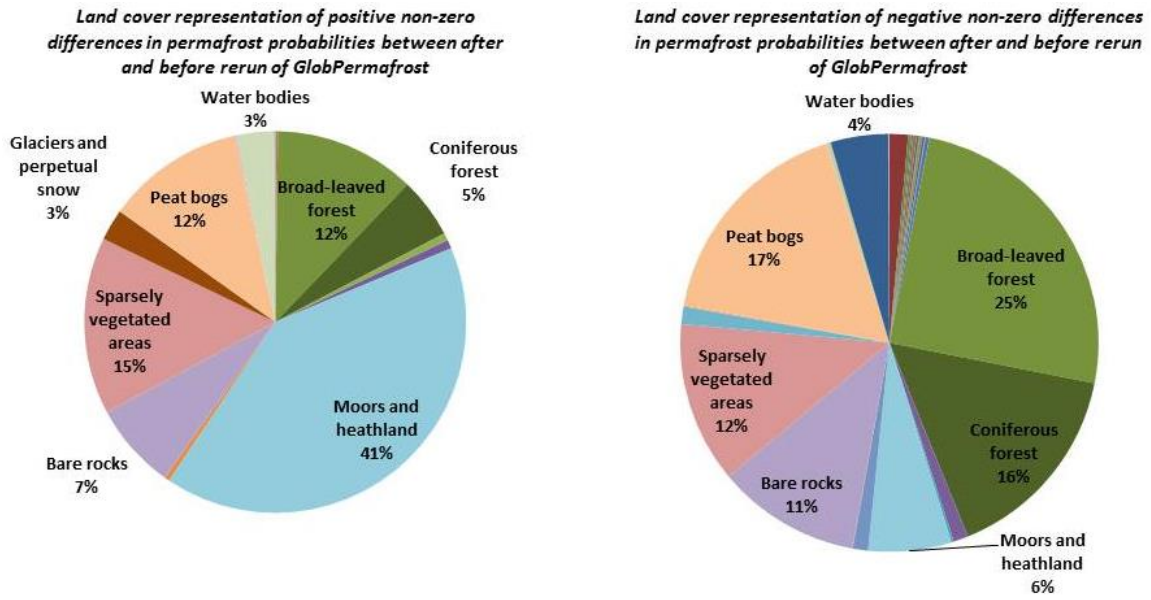

Figure 13 Land cover representation in areas with: positive differences in permafrost probabilities before and after rerun of the model, where there is more permafrost after the rerun than before (left); negative differences in permafrost probabilities before and after rerun of the model, where there is more permafrost before the rerun of the model than after (right).

The reduction of permafrost (the positive non-zero difference) after the rerun of the model occurred mainly in moors and heathlands which cover 41% of all areas with reduction (Fig. 13). However, the gain (the negative non-zero differences) of permafrost is found in forests (broad-leaved and coniferous) also covering 41% of all areas with gain of permafrost.

The GlobPermafrost model employs subcell statistics of land cover groups (more detailed in section 3.2). Since the wetland group (including inland marshes, salt marshes and peat bogs land cover classes of Corine 2012) plays an important role in determining permafrost occurrence in the model, we estimated wetland fraction per each MODIS cell for Corine (as it is performed for all land cover classes in subcell statistic estimation) and CCI land cover classes. Non-zero differences between wetland fractions in the Corine and the CCI land cover classes are plotted in Figure 15. Histograms of positive and negative differences look very similar. Areas with negative differences (i.e. where wetland fraction in Corine is higher than in CCI) tend to be located in the mountains, while the positive differences (i.e. with higher wetland fraction in CCI) are located both in the mountains as well as in lowlands areas.

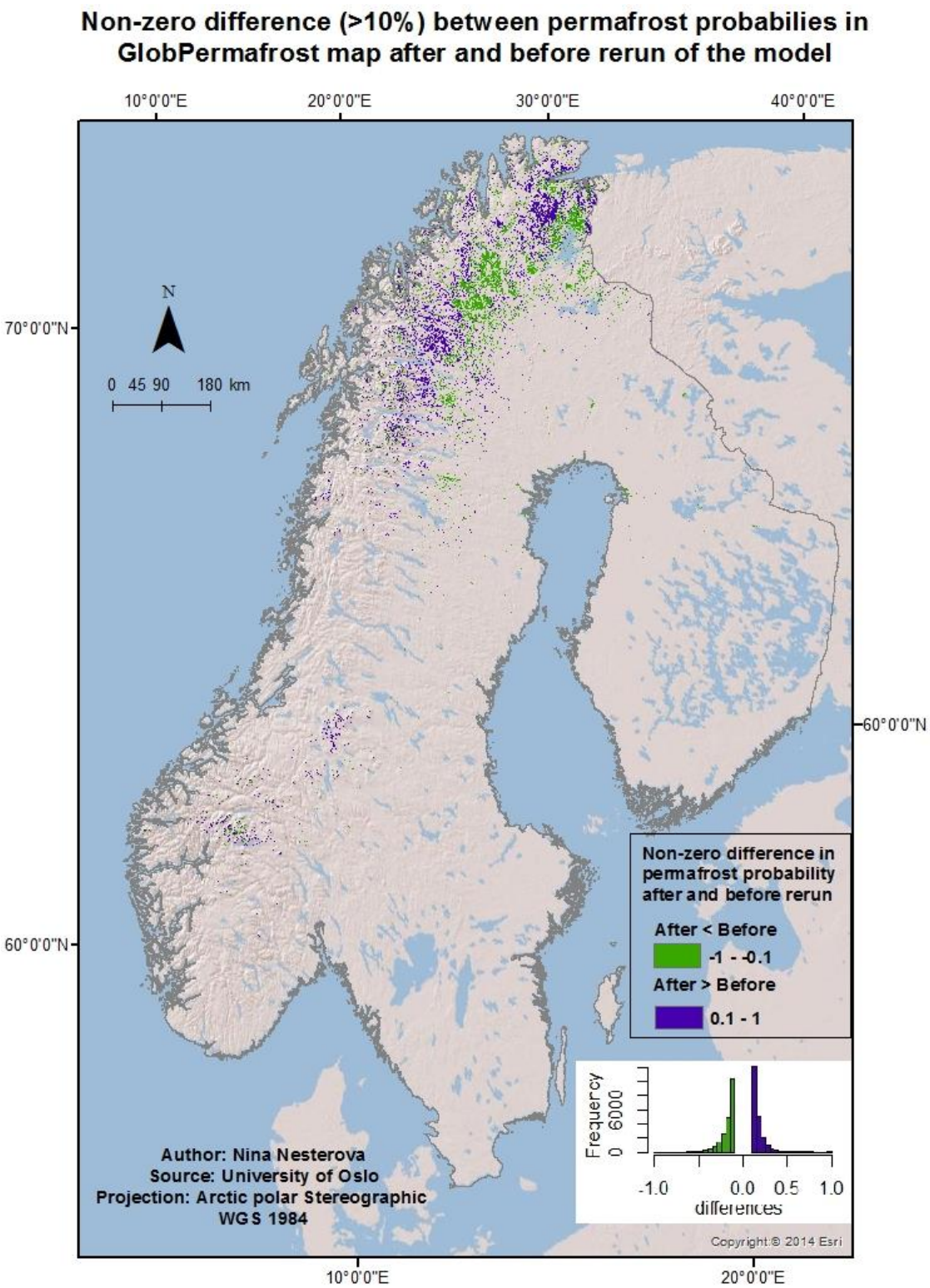

Figure 14 Map of the study area showing areas of differences (>10%) between the GlobPermafrost map before the rerun of the model and after. Purple denotes positive differences where there is more permafrost in the GlobPermafrost map after the rerun than in the GlobPermafrost map before the rerun. Green indicates negative differences where there is more permafrost in GlobPermafrost map before the rerun of the model than after. The histogram depicts the distribution of positive and negative differences.

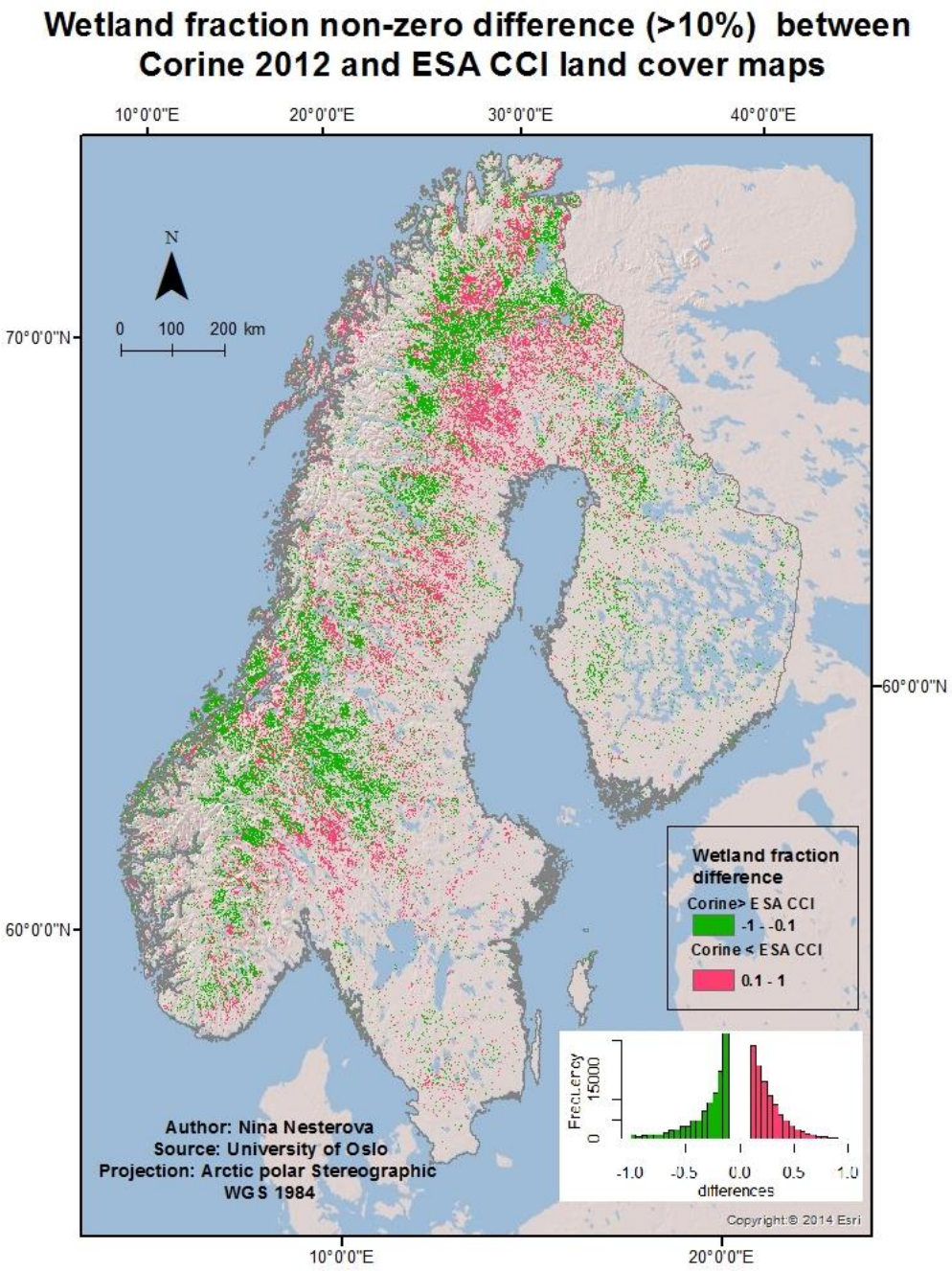

Figure 15 Map of the study area showing areas of differences (>10%) between wetland fraction in Corine 2012 and ESA CCI for 1 km grid cells. Pink denotes areas with bigger wetland fraction in Corine compared to ESA CCI land cover dataset. Green indicates areas with bigger wetland fraction In ESA CCI than in Corine land cover dataset. The histogram depicts the distribution of positive and negative differences.

Since wetlands play an important role in defining permafrost occurrence, we estimated how the distribution of differences in wetland fraction between Corine and CCI land cover maps influence the distribution of differences in the GlobPermafrost map permafrost probabilities before and after rerun of the model (Figure 16). There is a clear positive trend between these two distributions.

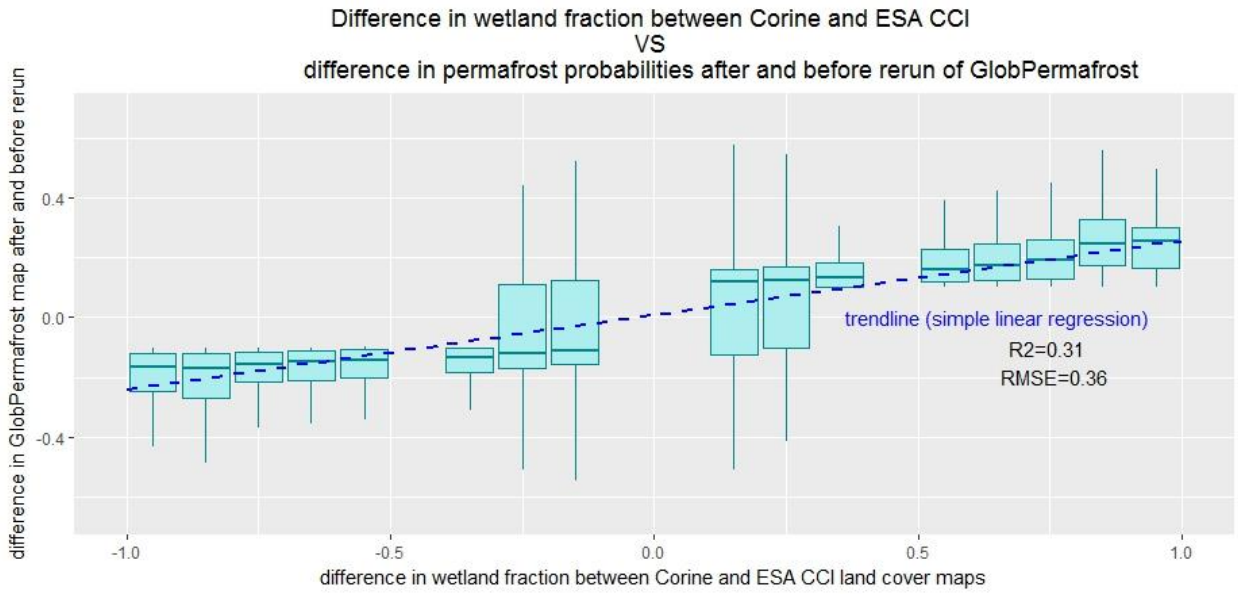

Figure 16 Differences in wetland fraction in Corine and CCI land cover datasets plotted against differences in permafrost probabilities in GlobPermafrost map after and before rerun of the model. Outliers are masked out in this plot. Green bars represent variation and their tips show the greatest and the lowest values without outliers. Horizontal line within boxes represents the median (50% of the data).

A simple linear regression model fitted to this dependency shows extremely low p-value (<2.2e-16) and relatively high r^2 (0.31). This means that differences in wetland fraction are a statistically significant predictor of differences in permafrost probabilities of the GlobPermafrost map after and before rerun, describing 30% of variation.

5 DISCUSSION

The results of the initial comparison between the regional permafrost map and the GlobPermafrost map point out the importance of different forcing data, which resulted in the disagreement between the two TTOP models.

Second comparison performed after rerun of GlobPermafrost with different land cover map indicates the significance of wetland fraction defining changes in permafrost probabilities after rerun of the model.

5.1. Performance of GlobPermafrost on regional scale of Scandinavia

5.1.1 Permafrost in forests

Permafrost occurrence in forests was widely distributed in regional permafrost map. Fig. 8 shows that the third highest mean value of permafrost probability belongs to broad-leaved forests.

Occurrence of permafrost (permafrost probabilities >0.1) in forests in all three maps is depicted on Fig. 17.

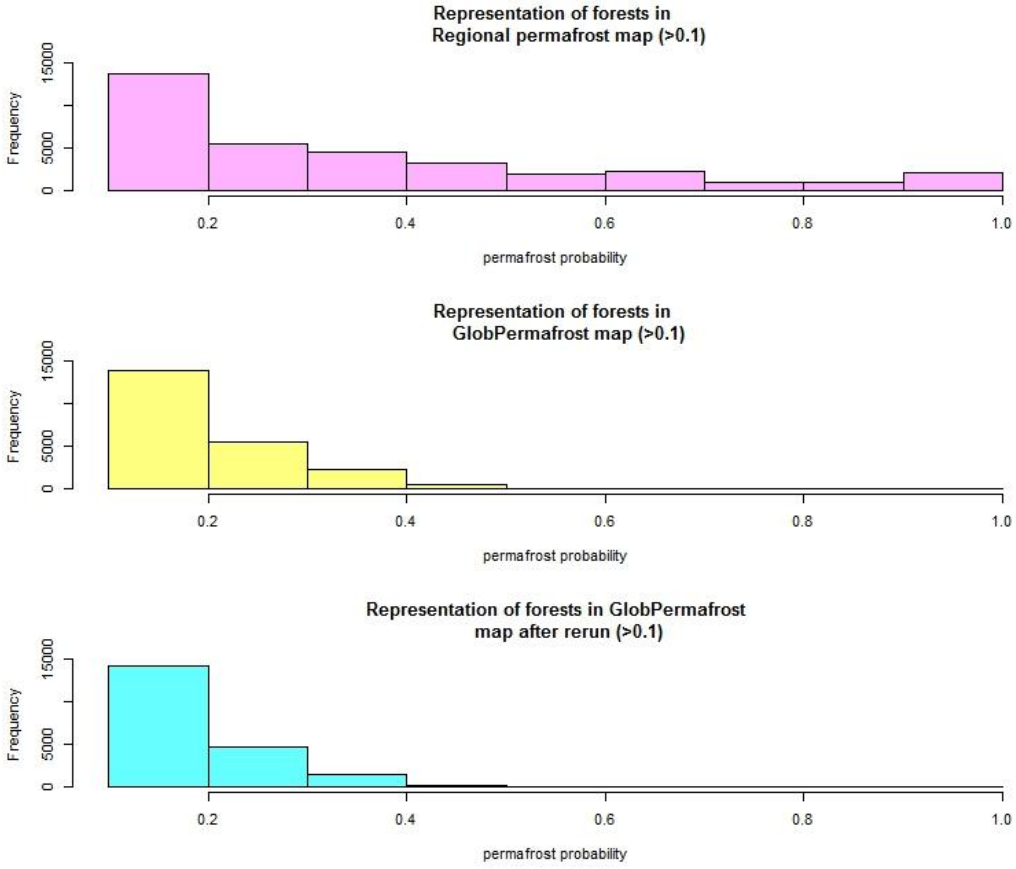

Figure 17 Occurrence of permafrost in forests (coniferous, mixed and broad-leaved): in regional permafrost map (where Corine land cover was used as an input; top), original GlobPermafrost map (where CCI land cover was used as an input; middle), GlobPermafrost map after model rerun (where Corine land cover was used as an input; bottom).

The whole range of permafrost probabilities in the regional permafrost map is found in areas covered by forests, but this is not the case for the GlobPermafrost maps. This corresponds to the fact that a quarter of all negative differences (where there is more permafrost in regional map than in GlobPermafrost) is located in forests (Fig. 7).

However, permafrost occurrence in Scandinavian forests was not reported by other researchers. For example, Johansson et al. (2006) described the role of forests (sparse birches) in Torneträsk region (Northern Sweden) as insulator for snow which leaded to the absence of permafrost. In contrast, permafrost was found in the areas covered by tundra vegetation, bare rock areas and in peat mires.

Permafrost occurrence in Finnmark (northern Norway) was described by Borge et al. (2017). This study focused on palsas and peat plateaus as main landforms determined by permafrost occurrence in this region. One of the results of this research was the map of palsa and peat plateaus distribution (Fig 18).

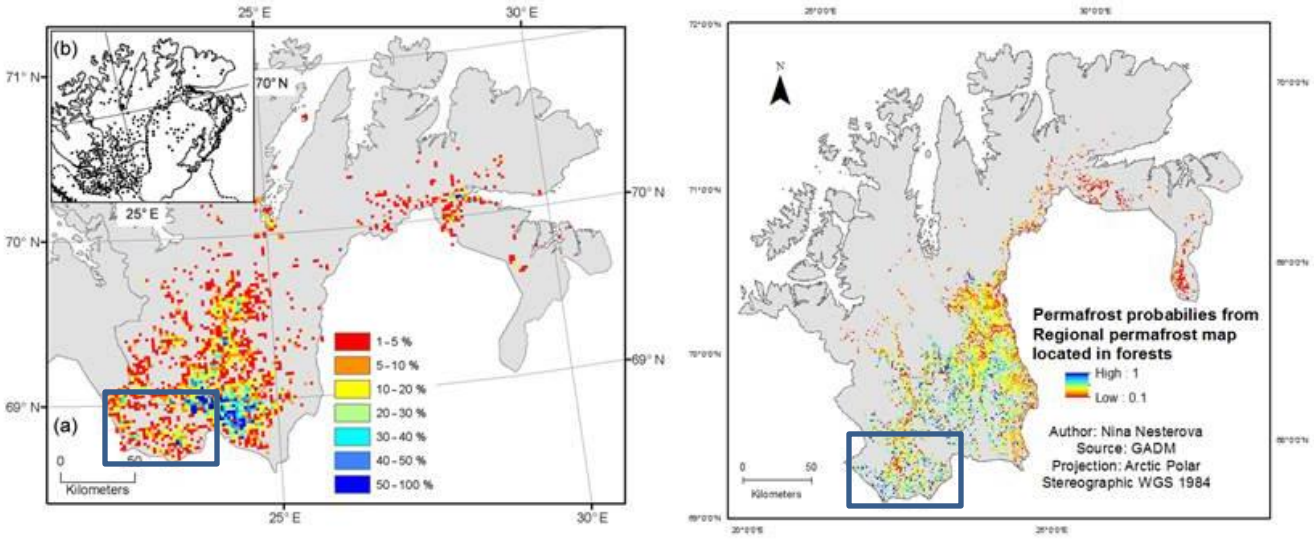

Figure 18 Distribution of palsas and peat plateaus in Finnmark, Northern Norway (Borge et al. 2017) (left). Access permission: Creative Commons Attribution 3.0 License;
Permafrost probabilities from regional permafrost map located in forests in Finnmark, Northern Norway (right).

Permafrost in the south of Finnmark is reported to be found in form of palsa and peat plateaus while the regional permafrost model predicts permafrost in forests: i.e. selected are has high values of palsa occurrence according to Borge et al. (2017) and at the same time high values of permafrost occurrence in forests predicted by the regional model (Fig. 18). This fact may lead to the conclusion that the regional permafrost model does not represent trustworthy permafrost occurrence in forest areas. However, GlobPermafrost does represent much smaller range of permafrost probabilities, the majority of which has low values.

The reason might be the different treatment of snow distribution in the two models. In the regional permafrost model, coefficient of variation affecting snow distribution is fixed to 7 (Fig. 1). However, in the GlobPermafrost model coefficient of variation is estimated for every proportion of land cover representation according to subcell statistics (Fig. 2 and Table 1).

Despite the fact that the GlobPermafrost map shows less permafrost in forests, it still does predict it. For example, 18% of all areas where there is more permafrost in GlobPermafrost compared to regional map are covered by forests (Fig. 7). This could occur because no corrections were applied for converting MODIS LST measured in forests (which are top-of-canopies temperatures) to ground surface temperature under canopies. Moreover, approximately 41% of areas of permafrost gained after the rerun of GlobPermafrost model with Corine land cover were also found in forests (Fig. 13). This may originate from different distribution of forests in Corine and ESA CCI land cover datasets.

To summarize, both models represent permafrost occurrence in forests. However, since there is substantially smaller amount of permafrost predicted by the GlobPermafrost model, in specific case of permafrost predictions in forests, the GlobPermafrost model may be more trustworthy for this particular land cover type.

5.1.2 Permafrost in the mountains

Dominance of sparsely vegetated areas, bare rocks, moors and heathland land cover classes in the context of permafrost probabilities can be explained by the fact that they are mostly located in mountainous areas where other factors (i.e. FDD, TDD and thin snow cover) may play a large role. Thus, more permafrost may occur in areas with these land cover classes. This corresponds to prevalence of these classes in different plots (see mean value of permafrost probability in regional map for Sparsely vegetated areas in Fig. 8, difference plotted in Fig. 7, Fig. 12, Fig. 13).

5.1.3 Permafrost in wetlands

Wetlands are important in determining permafrost occurrence. Non-mountainous permafrost in the northern Fennoscandia region is mostly located in mires and peat areas (as described in 2.2.2), this corresponds to low rk-value in the model assigned for wetlands group, where peat bogs belong to. This leads to relatively high mean values of permafrost occurrence in peat bogs (Fig. 8).

Histograms in Fig. 19 depict representation of wetlands in areas with permafrost occurrence higher than 10% (>0.1 permafrost probability). Different permafrost probabilities can be found in regional permafrost map with peaks at lowest and at highest values.

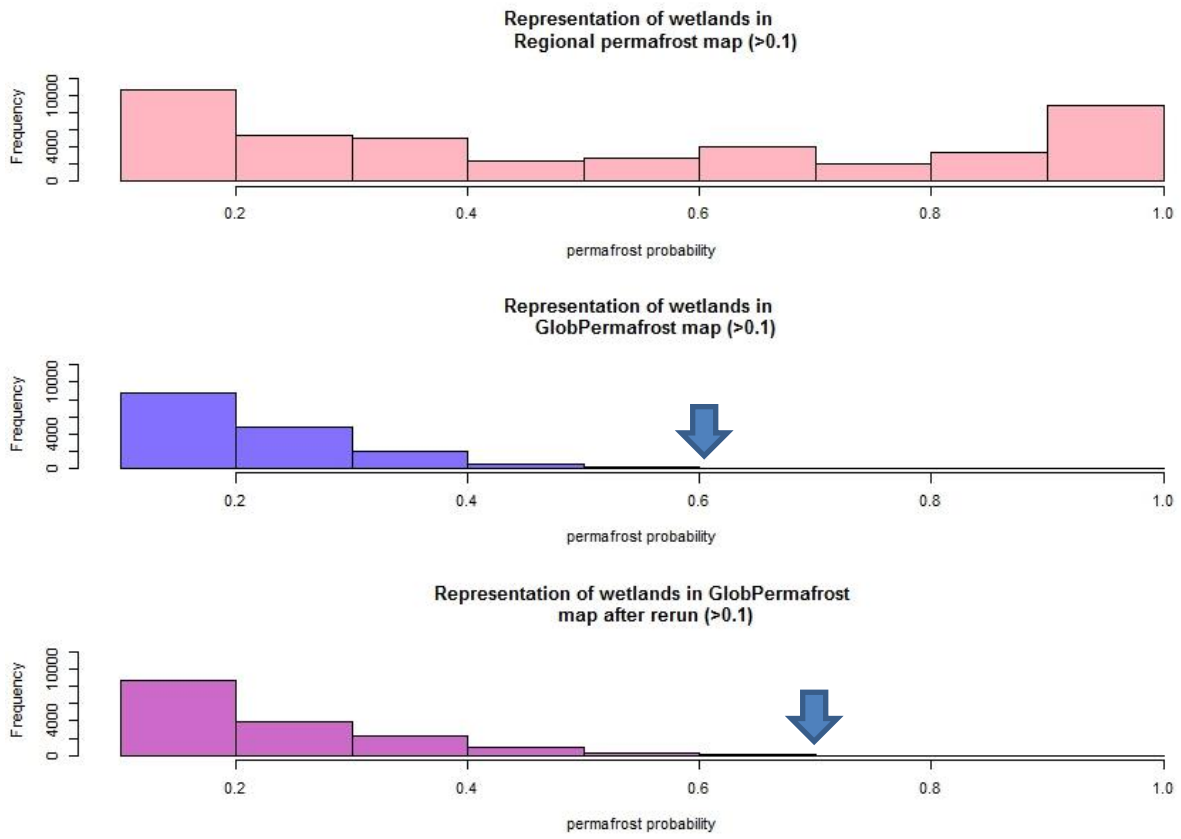

Figure 19 Occurrence of permafrost in wetlands: in regional permafrost map (top), original Globpermafrost map (middle), GlobPermafrost map after the model rerun (bottom). Blue arrows indicate maximum of permafrost probabilities.

The expected gain of permafrost probability in wetlands after GlobPermafrost model rerun was identified but was not significant and hardly visible on the graph (blue arrows).

The wetland fraction distribution difference between CCI and Corine land cover maps (Fig. 19) had a little influence on the differences in permafrost probabilities between regional and GlobPermafrost maps (Fig. 6). Fitted simple linear regression model showed r^2 value equaled to 0.07. This means that only 7% of disagreement between regional map and GlobPermafrost can be explained by wetland fraction differences. Therefore the other factors contributed significantly more to disagreements between regional and GlobPermafrost maps.

5.1.4 Factors influencing the performance of the GlobPermafrost on regional scale of Scandinavia

There are several differences in initial setups of regional permafrost model and GlobPermafrost model, which resulted in disagreements between their output maps.

Table 3 Comparison of data used to assign n-factors and define freezing and thawing degree days

	Data used to assign parameters	
	Regional permafrost model (Gisnas et al. 2017)	**GlobPermafrost model (GlobPermafrost initiative of European Space Agency)**
rk-factors	Joint sediment maps of Norway, Sweden and Finland (Olesen et al. 2010) Thermal properties used in the model GIPL 1.0 (Geophysical Institute Permafrost Laboratory, University of Alaska, Fairbanks)	Tundra wetness data by Widhalm et al. (2016) ESA CCI land cover (period 2008 - 2012, version 1.6.1)
nf-factor	Nordic Gridded Climate Dataset (Norwegian Meteorological Institute, Oslo) air temperatures Nordic Gridded Climate Dataset (Norwegian Meteorological Institute, Oslo) precipitations Corine land cover 2012 (Aune-Lundberg and Strand, 2010)	MODIS LST (product level 3, version 6) ERA-interim precipitations ERA-interim air temperatures
nt-factor	Nordic Gridded Climate Dataset (Norwegian Meteorological Institute, Oslo) Corine land cover 2012 (Aune-Lundberg and Strand, 2010)	Not applied
Freezing degree days (FDD) and thawing degree days (TDD)	Nordic Gridded Climate Dataset (Norwegian Meteorological Institute, Oslo) air temperatures Nordic Gridded Climate Dataset (Norwegian Meteorological Institute, Oslo) precipitations	MODIS LST (product level 3, version 6) ERA-interim air temperatures

A comparison among different data used to assign model parameters in Regional and GlobPermafrost permafrost models is shown in the Table 3. One crucial difference in forcing data belongs to origins of temperature data.

Temperature data had an influence on defining nt and nf functions, which account for surface offset between air temperature and ground surface temperature (detailed in section 2.3.1). In the regional model, air temperatures from the Nordic Gridded Climate Dataset were interpolated and used in empirically derived equation to estimate nf-factors for open areas. The same procedure was applied to compute nt-factors.

Nt-factors were omitted in the GlobPermafrost model because MODIS LST combined with ERA-interim air temperatures were assumed to satisfactory represent ground surface temperatures. However, nf-factors were calculated from the fusion of both datasets. MODIS satellite data represent surface temperature, which not always represents the true ground surface, but, for example forest canopies. This case of uncertainty was described in section 5.1.1.

Precipitation data is assumed to have smaller impact on the detected differences between the two models. However, the Nordic Gridded Climate Dataset has significantly higher initial resolution (1 km^2) compared to ERA-interim reanalysis data (6400 km^2). Moreover, the Nordic

Gridded Climate Dataset is based on local weather station data which is probably more robust than reanalysis data.

5.2 The role of land cover in TTOP model

The main aim of the rerun of the GlobPermafrost model with Corine 2012 land cover was to study the role of land cover in TTOP model.

The Corine 2012 land cover has 3 times higher spatial resolution compared to ESA CCI. The performance of the GlobPermafrost was expected to be improved with Corine 2012 land cover. However, relatively similar values of r^2 indicate no substantial change in the model performance: nor better, nor worse. The expected improvements of model output as a result of the improved land cover input did not occur.

One of the reasons for such expectations was an assumption of Corine 2012 land cover data to represent more wetlands as well as more accurate distribution of them.

However, as shown on Fig. 15 (histograms) negative and positive differences between wetland fraction in Corine 2012 and ESA CCI are relatively similarly distributed. This means that approximately the same amount of pixels where ESA CCI has higher wetland fraction than Corine can be described vice versa: expected gain in wetland fraction was compensated by the loss of wetland fraction. Moreover, a lot of negative wetland fraction differences occurred too far on the south of study area, where permafrost already could not occur.

Absence of a great change of GlobPermafrost performance before and after rerun of the model points out the minor role of land cover in TTOP model. In contrast this result indicates the importance of other factors (such as nf-factors, FDD and TDD) used in regional model causing differences between regional permafrost and GlobPermafrost maps.

5.3 Sources of uncertainty

The result of the GlobPermafrost model run with Corine land cover inherits majority of uncertainties belonged to the initial GlobPermafrost setups. Main uncertainties in GlobPermafrost are caused by forcing data (Fig. 2).

Main errors from MODIS LST are related to MODIS instrument itself and LST algorithm (Wan 1999). Evaluation of MODIS LST ability to represent near surface air temperatures in Northern China performed by Yang et al. (2017) showed high accuracy of LST, varying from good performance in plains to worse in complex terrains and mountains.

One of the major factors of uncertainty from ERA-interim reanalysis in climate data for the study area is related to limited amount of direct temperature measurements in the Arctic (Copernicus Climate Change Service, ECMWF, 2015). Relatively high agreement in the Arctic temperature fluctuations was found with JRA-55 reanalysis data together with in-situ measurements in Arctic (Poli and Simmons 2015). In general ERA-interim reanalysis in climate data was assumed to reasonably represent global climate data (Copernicus Climate Change Service, ECMWF, 2015).

Uncertainties associated with ESA CCI land cover data also contribute to general inaccuracy of GlobPermafrost map. Validation of ESA CCI land cover data was performed by comparison with GlobCover 2009, another satellite based land cover data. Thus, no field validation of these data was applied. Moreover, land cover classes in the study area (for example: sparsely vegetated areas, lichens and mosses, mixed and mixed broadleaved and needle leaved forests) are reported to have low accuracy (Land Cover CCI PRODUCT USER GUIDE VERSION 2.0, 2017).

Assessment of Corine 2012 land cover accuracy was performed based on more than 25000 validation points at pan-European level as well as at the level of European Biogeographical regions. Apart from different validation approaches, available in-situ data were also used. Overall accuracy was reported to be 81.8%.

Thus, we can conclude that replacing ESA CCI land cover with Corine 2012 land cover data would probably decrease the uncertainty of GlobPermafrost result if the land cover component was one of the most important input data.

5.4 Limitations of TTOP approach

Several studies were conducted successfully applying TTOP model within the study area of this paper (Gisnas et al. 2013; Westermann et al. 2015b). However, the TTOP approach is an equilibrium model, which has several limitations (Zhang et al. 2014). The main shortcoming of TTOP is in the assumption of ground thermal properties being in equilibrium with climate and doesn't take into account the time-lag in the impact of climatic influence (Callaghan et al. 2011). Moreover, Osterkamp (2005) and Zhang et al. (2008) described a disequilibrium nature of permafrost thermal conditions in response to climate forcing.

Westermann et al. (2013) applied a transient model to estimate thermal conditions in southern Norway. More complex and sophisticated transient models are assumed to have high predictive capacity. Instead of fixed parameters for soil properties, as in the case of equilibrium approach, transient models estimate variation of these parameters within certain time intervals (Callaghan et al. 2011). However, because of big input data requirements (i.e. vegetation information, ground conditions, carbon and ice content in the soil, atmospheric information, etc.) and computational complexity, such models are not widely implemented for big areas (Zhang et al. 2008).

An important limitation of both equilibrium and transient approaches is related to deterministic modeling scheme, when the nature of permafrost parameters is rather stochastic (Callaghan et al. 2011). To overcome this issue, a probabilistic modeling approach was developed.

In permafrost modeling in the North Atlantic region (Westermann et al. 2015b) equilibrium TTOP model was incorporated with statistical modeling by applying combinations of parameters from a certain range. The same scheme was implemented in both GlobPermafrost (Obu et al. in prep.) and regional permafrost models (Gisnas et al. 2017).

Low computation requirements, availability of input data, small number of parameters and robustness are advantages of the TTOP approach over the transient approach. On the continental scale application TTOP model was assumed to be more reasonable compared to more advanced models (Westermann et al. 2015b).

5.5 Further study

5.5.1 Spatial analysis of initial disagreement

Due to time limits, several steps of analysis of initial disagreement had to be omitted. More detailed investigation of non-zero differences distribution may help to discover new patterns and relations. That would be valuable to explore spatial correlation of non-zero differences with respect to North and South, elevation, exposition or slopes. Moreover, it would be interesting to find out where exactly in mountains disagreements tend to have higher values.

Statistical analysis of clustering of non-zero differences would give an opportunity to find out the most problematic areas.

5.5.2 Sensitivity of GlobPermafrost to other parameters

To find the main cause of disagreements between regional and GlobPermafrost maps, the roles of other inputs in TTOP model should be investigated. Sensitivity of GlobPermafrost to different approaches in defining rk-factors will give an indication of which of them can lead to lower uncertainty.

It would be meaningful to explore how calculating FDD and TDD from different temperature data sources (MODIS satellite LST and weather stations) affect the result. This could be done, for example, by rerunning GlobPermafrost for Scandinavia with Nordic Gridded Climate Data.

Another opportunity to explore the role of land cover in TTOP (apart from the one applied) can be changing the approach of grouping land cover classes in the rerun of GlobPermafrost. Transitional wood-shrub class of Corine land cover was classified as shrubs. However, the description of this class states the presence of young and grown-up trees. Thus, it would be interesting to check if relocating this land cover class to another group would influence the result and if there is a need to set up new intermediate group.

5.5.3 Global perspective

Since GlobPermafrost map covers circum-Arctic region, there are many other regions that can be studied. The important role of wetland fraction in defining the result was described in section 4.2. However, wetlands are not numerous in Scandinavia. Thus, performing this experiment in the region of western Siberia may give profound result making this research more comprehensive.

Investigation of GlobPermafrost predictions over the places with documented permafrost landforms (i.e. palsa and pingos) occurrence and its relation to Corine land cover classes can be a separate topic of research.

Different research ideas stated above are just some of research opportunities which can help to improve the performance of permafrost models in general and TTOP performance in particular.

6 CONCLUSIONS

This study represents the analysis of the GlobPermafrost model performance for Scandinavia and the role of land cover as input to this model.

Initial comparison of the GlobPermafrost map with the regional permafrost map showed overall an underestimation of permafrost occurrence in Scandinavia. The lowest underestimations were located in regions with little permafrost, while the highest underestimations were found in mountainous and wetland areas where permafrost occurrence is more likely.

Improved input land cover data did not greatly affect the performance of the GlobPermafrost with small changes significantly caused by difference in wetland fraction between the two input land cover data. Substantial differences in wetland fractions were located in the south of the study area and, thus, were not translated into permafrost. However, this may significantly vary for other regions of the Arctic. The difference in wetland fraction of land cover datasets (for i.e. Siberia or Canada) can originate from areas with environmental conditions which are already very likely to contribute to permafrost occurrence.

The minor role of land cover in TTOP model found in this study indicates great importance of other input data such as i.e. climatic forcing data. This conclusion can assist in the directions taken for future studies and improvements in permafrost modeling.

7 REFERENCES

Alfred-Wegener-Institut. ESA DUE GlobPermafrost Arctic. Retrieved 01.02.2018 2018, from. http://maps.awi.de/map/

Anonymous. 2014. LANDSCAPES, CLIMATIC ZONES AND OPTIMAL AGRARIAN AREAS IN SCANDINAVIA. *Acta Archaeologica*, 85**:** 8.

Aune-Lundberg, L., and G. H. Strand, 2010. CORINE Land Cover 2006. The Norwegian CLC2006 project. Norwegian Forest and Landscape Institute Report 8231101144. [in Swedish, English summary]

Baranov, I. Y., and R. National Research Council of Canada. Division of Building, 1964. Geographical Distribution of Seasonally Frozen Ground and Permafrost. National Research Council Canada Report 0077-5606. [in Swedish, English summary]

Borge, A. F., S. Westermann, I. Solheim, and B. Etzelmüller. 2017. Strong degradation of palsas and peat plateaus in northern Norway during the last 60 years. *The Cryosphere, Vol 11, Iss 1, Pp 1-16 (2017)***:** 1. DOI: 10.5194/tc-11-1-2017

Brown, J., O. J. Ferrians Jr., J. A. Heginbottom, and E. S. Melnikov. 1997. *Circum-Arctic map of permafrost and ground-ice conditions*. US Geological Survey Reston.

Callaghan, T., M. Johansson, R. D. Brown, P. Y. Groisman, N. Labba, and R. V. 2011. Changing Snow Cover and its Impacts. In *Snow, Water, Ice and Permafrost in the Arctic (SWIPA): Climate Change and the Cryosphere*. Arctic Monitoring and Assessment Programme (AMAP).

Etzelmuller, B., I. Berthling, and J. L. Sollid. 2003. Aspects and concepts on the geomorphological significance of Holocene permafrost in Southern Norway. *Geomorphology*, 52**:** 87-104. DOI: 10.1016/S0169-555X(02)00250-7

Gisnas, K., B. Etzelmuller, H. Farbrot, T. V. Schuler, and S. Westermann. 2013. CryoGRID 1.0; permafrost distribution in Norway estimated by a spatial numerical model. *Permafrost and Periglacial Processes*, 24**:** 2-19. DOI: 10.1002/ppp.1765

Gisnas, K., B. Etzelmuller, C. Lussana, J. Hjort, A. B. K. Sannel, K. Isaksen, S. Westermann, P. Kuhry, et al. 2017. Permafrost map for Norway, Sweden and Finland. *Permafrost and Periglacial Processes*, 28**:** 359-378. DOI: 10.1002/ppp.1922

Gruber, S. 2012. Derivation and analysis of a high-resolution estimate of global permafrost zonation. *The Cryosphere, Vol 6, Iss 1, Pp 221-233 (2012)***:** 221. DOI: 10.5194/tc-6-221-2012

IPA. International Permafrost Association. Retrieved 03.03.2018 2018, from. https://ipa.arcticportal.org/

Isaksen, K., P. Holmlund, J. L. Sollid, and C. Harris. 2001. Three deep alpine-permafrost boreholes in Svalbard and Scandinavia. *Permafrost and Periglacial Processes*, 12**:** 13-25.

Johansson, M., T. R. Christensen, H. J. Akerman, and T. V. Callaghan. 2006. What determines the current presence or absence of permafrost in the Tornetrask region, a sub-arctic landscape in northern Sweden? *Ambio*, 35**:** 190-197.

Jorgenson, M. T., and G. Grosse. 2016. Remote sensing of landscape change in permafrost regions. *Permafrost and Periglacial Processes*, 27**:** 324-338. DOI: 10.1002/ppp.1914

King, L. 1986. Zonation and ecology of high mountain permafrost in Scandinavia. *Geografiska Annaler. Series A: Physical Geography*, 68**:** 131-139.

Lidmar-Bergström, K., and J. O. Näslund. 2005. Major landforms and bedrock. In *The Physical Geography of Fennoscandia*, 3-16 pp. Oxford: Oxford University Press.
Network-CALM, C. A. L. M. Long-Term Observations of the Climate-Active Layer-Permafrost System. Retrieved 05.05.2018 2018, from. https://www2.gwu.edu/~calm/
Obu, Westermann, Kääb, and Bartsch. Ground temperature and permafrost maps of the Northern Hemisphere based on remote sensing and reanalysis data.
Olesen, O., M. Brönner, J. Ebbing, J. Gellein, L. Gernigon, J. Koziel, T. Lauritsen, R. Myklebust, et al. 2010. New aeromagnetic and gravity compilations from Norway and adjacent areas: methods and applications. In *Geological Society, London, Petroleum Geology Conference series*, 559-586. Geological Society of London.
Onuchin, A. A., and T. A. Burenina. 1996. Climatic and geographic patterns in snow density dynamics, Northern Eurasia. *Arctic and Alpine Research***:** 99-103.
Osterkamp, T. E. 2005. The recent warming of permafrost in Alaska. *Global and Planetary Change*, 49**:** 187-202. DOI: 10.1016/j.gloplacha.2005.09.001
Pidwirny, M. 2006. Fundamentals of physical geography. *Date Viewed*, 19**:** 2009.
Poli, P., and A. J. Simmons. 2015. Arctic warming in ERA-Interim and other analyses. *Quarterly Journal of the Royal Meteorological Society*. DOI: 10.1002/qj.2422
Seppälä, M. 2005. Periglacial environment. In *The Physical Geography of Fennoscandia*, 349-364 pp.: Oxford University Press.
Service, C. C. C., 2015. Uncertainties in ERA-Interim. ECMWF Report. [in Swedish, English summary]
Skaugen, T., E. Alfnes, E. G. Langsholt, and H. C. Udnæs. 2004. Time-variant snow distribution for use in hydrological models. *Annals of Glaciology*, 38**:** 180-186.
Smith, M. W., and D. W. Riseborough. 1996. Permafrost monitoring and detection of climate change. *Permafrost and Periglacial Processes*, 7**:** 301-309.
Tikkanen. 2005. Climate. In *The Physical Geography of Fennoscandia*. Oxford: Oxford University Press.
UCL-GEOMATICS. 2017. Land Cover CCI. Product User Guide Version 2.0 (CCI-LC-PUGV2).
Wan, Z. 1999. MODIS land-surface temperature algorithm theoretical basis document (LST ATBD). *Institute for Computational Earth System Science, Santa Barbara*, 75.
Westermann, S., C. R. Duguay, G. Grosse, and A. Kääb. 2015a. Remote sensing of permafrost and frozen ground. *Remote Sensing of the Cryosphere***:** 307-344.
Westermann, S., T. I. Østby, K. Gisnås, T. V. Schuler, and B. Etzelmüller. 2015b. A ground temperature map of the North Atlantic permafrost region based on remote sensing and reanalysis data. *The Cryosphere, Vol 9, Iss 3, Pp 1303-1319 (2015)***:** 1303. DOI: 10.5194/tc-9-1303-2015
Westermann, S., T. V. Schuler, K. Gisnas, and B. Etzelmuller. 2013. Transient thermal modeling of permafrost conditions in Southern Norway. *Cryosphere [Online]*, 7**:** 719-739.
Widhalm, B., A. Bartsch, M. B. Siewert, G. Hugelius, B. Elberling, M. Leibman, Y. Dvornikov, and A. Khomutov. 2016. Site scale wetness classification of tundra regions with C-band SAR satellite data. In *Proceedings of the ESA Living Planet Symposium*.
Yang, Y. Z., W. H. Cai, and J. Yang. 2017. Evaluation of MODIS land surface temperature data to estimate near-surface air temperature in Northeast China. *Remote Sensing*, 9. DOI: 10.3390/rs9050410

Zhang, T., J. A. Heginbottom, R. G. Barry, and J. Brown. 2000. Further statistics on the distribution of permafrost and ground ice in the Northern Hemisphere. *Polar Geography [1995]*, 24**:** 126-131.

Zhang, T., I. Olthof, R. Fraser, and S. A. Wolfe. 2014. A new approach to mapping permafrost and change incorporating uncertainties in ground conditions and climate projections. *The Cryosphere, Vol 8, Iss 6, Pp 2177-2194 (2014)***:** 2177. DOI: 10.5194/tc-8-2177-2014

Zhang, Y., W. Chen, and D. W. Riseborough. 2008. Disequilibrium response of permafrost thaw to climate warming in Canada over 1850-2100. *Geophysical Research Letters*, 35. DOI: 10.1029/2007GL032117